41st ISYA Lecturer: *Gustavo Bruzual, IRyA, UNAM; Campus Morelia, México*

Topic: *GALAXIES (6 lectures)*

Description: An overview of the basic properties of galaxies due to the distribution, kinematics, dynamics, relevance, and evolution of their different stellar populations. A view of the basic properties and processes in the distant universe as revealed by galaxies of all types discovered so far.

Syllabus:

Lecture 1: **The Milky Way as a galaxy**
- The structure of the Galaxy
- The galactic disk
- The galactic bulge
- The galactic halo
- The galactic center
- Velocity of the sun
- Rotation curve of the Galaxy
- Stellar populations in the Galaxy

Lecture 2: **The world of galaxies (1)**
- Morphological classification. The Hubble Sequence
- Other types of galaxies
- Elliptical galaxies
- Spiral galaxies
- Galaxies in the local group
- Scaling relations

Lecture 3: **The world of galaxies (2)**
- The extragalactic distance scale
- The luminosity function of galaxies
- Black holes in the centers of galaxies
- Galaxies as gravitational lenses
- Stellar population synthesis
- Spectral evolution of galaxies
- Chemical evolution of galaxies

Lecture 4: **Clusters and groups of galaxies**
- The local group
- Galaxies in clusters and groups
- Morphological classification of clusters
- Spatial distribution of galaxies in clusters
- Luminosity function of cluster galaxies
- Clusters of galaxies as gravitational lenses
- Evolution of clusters

Lecture 5: **Galaxies at high redshift (1)**
- Lyman-break galaxies
- Starburst galaxies
- Extremely red objects
- Sub-millimeter sources
- Damped Lyman-alpha systems
- Lyman-alpha blobs
- Gamma-ray bursts

Lecture 6: **Galaxies at high redshift (2)**
- Background radiation
- Re-ionization of the universe
- Cosmic star formation history
- Galaxy formation and evolution

Requirements: Video projector in the class room

Bibliography:

- Schneider, *Extragalactic astronomy and cosmology*
- Sparke & Gallager, *Galaxies in the Universe*
- Mo, van den Bosch & White, Galaxy formation and evolution (selected chapters)

Clusters and Groups of Galaxies

Galaxy Cluster Abell 2218 **HST • WFPC2**

NASA, A. Fruchter and the ERO Team (STScI, ST-ECF) • STScI-PRC00-08

Galaxies are not uniformly distributed in space, but instead show a tendency to gather together in *galaxy groups* and *clusters of galaxies*. This effect can be clearly recognized in the projection of bright galaxies on the sky (see Figs. 6.1 and 6.2). The Milky Way itself is a member of a group, called the Local Group (Sect. 6.1), which implies that we are living in a locally overdense region of the Universe.

The transition between groups and clusters of galaxies is smooth. The distinction is made by the number of their member galaxies. Roughly speaking, an accumulation of galaxies is called a group if it consists of $N \lesssim 50$ members within a sphere of diameter $D \lesssim 1.5h^{-1}$ Mpc. Clusters have $N \gtrsim 50$ members and diameters $D \gtrsim 1.5h^{-1}$ Mpc. A formal definition of a cluster is presented further below. An example of a group and a cluster of galaxies is displayed in Fig. 6.3.

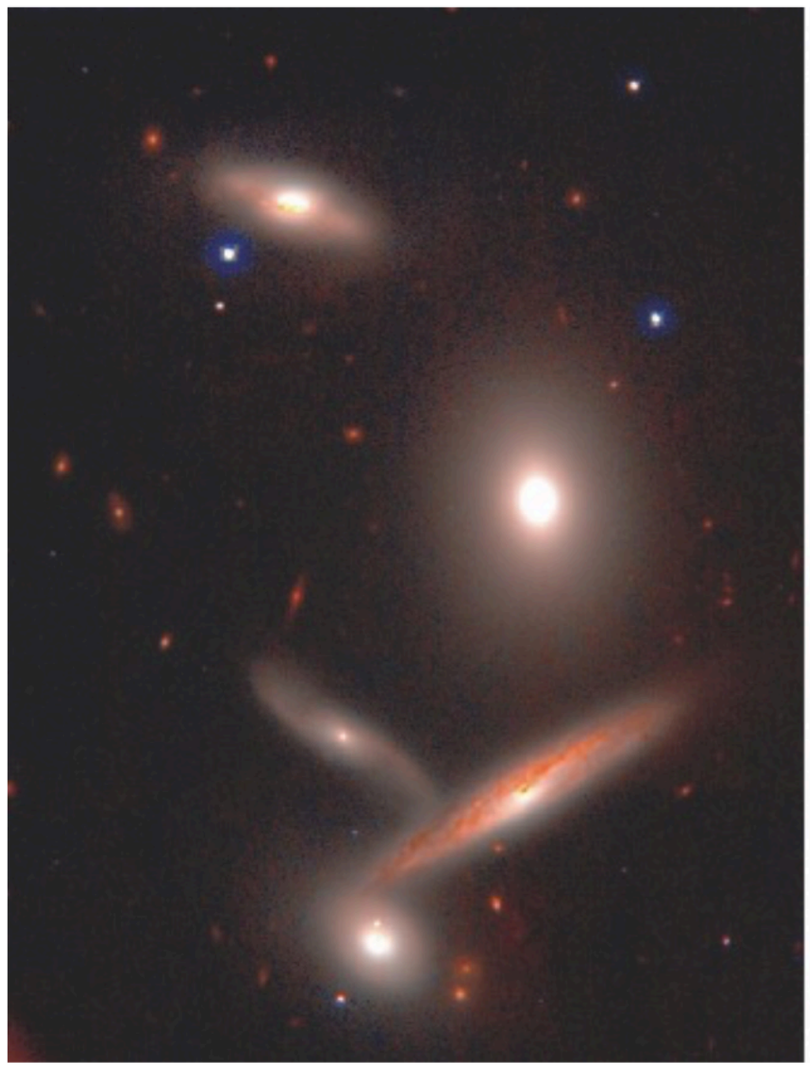

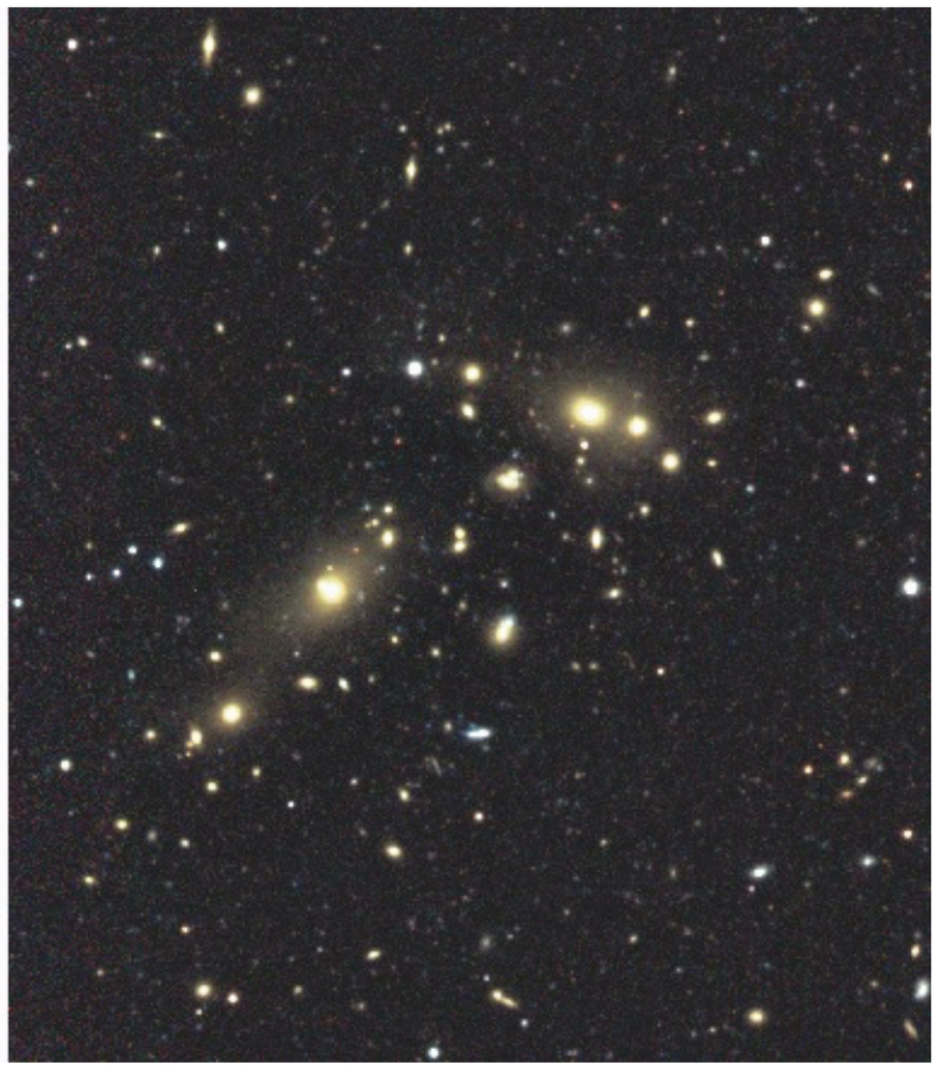

Fig. 6.3. Left: HCG40, a compact group of galaxies, observed with the Subaru telescope on Mauna-Kea. Right: the cluster of galaxies Cl 0053−37, observed with the WFI at the ESO/MPG 2.2-m telescope

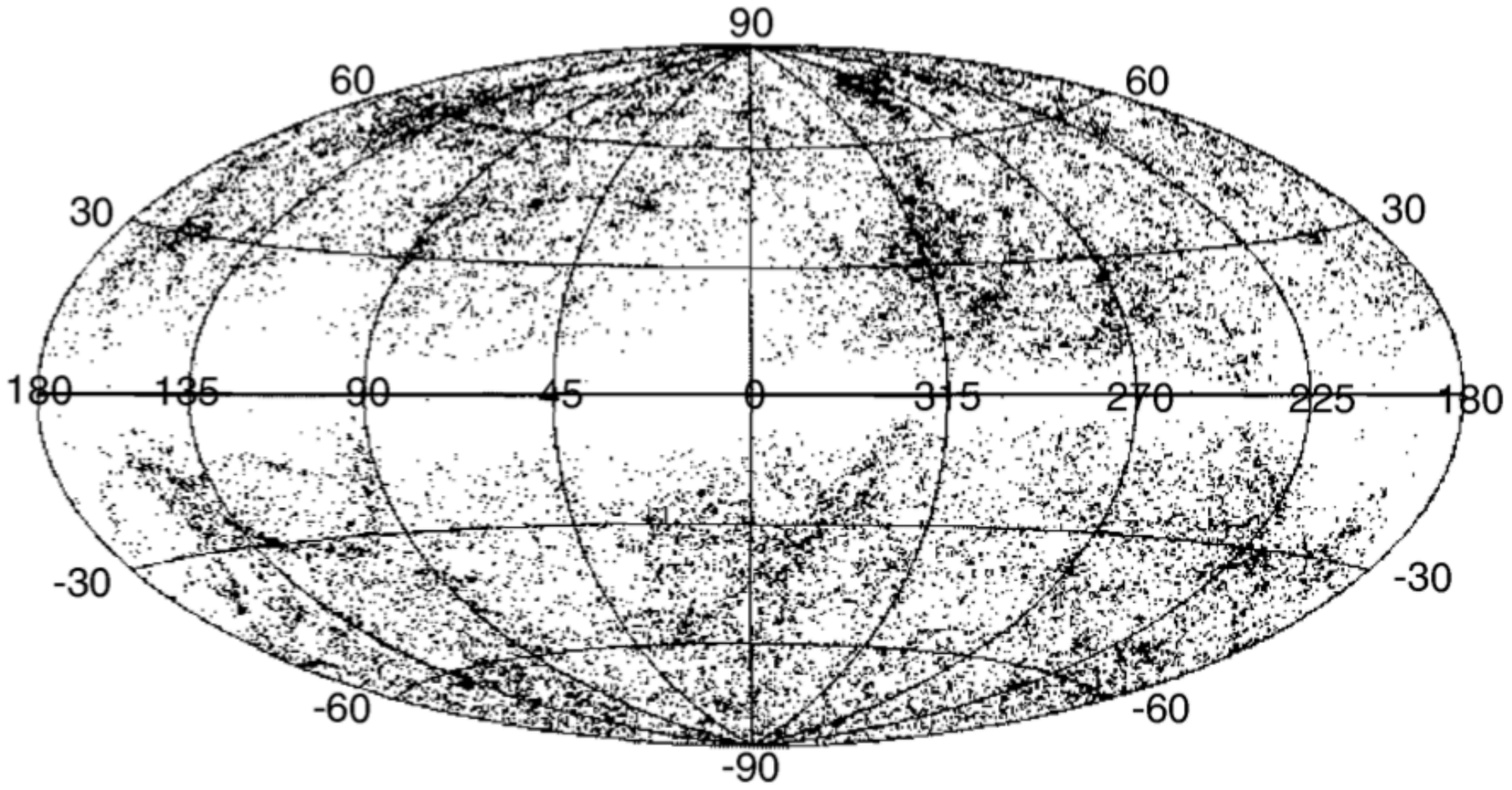

Fig. 6.2. The distribution of all galaxies brighter than $B < 14.5$ on the sphere, plotted in Galactic coordinates. The Zone of Avoidance is clearly seen as the region near the Galactic plane

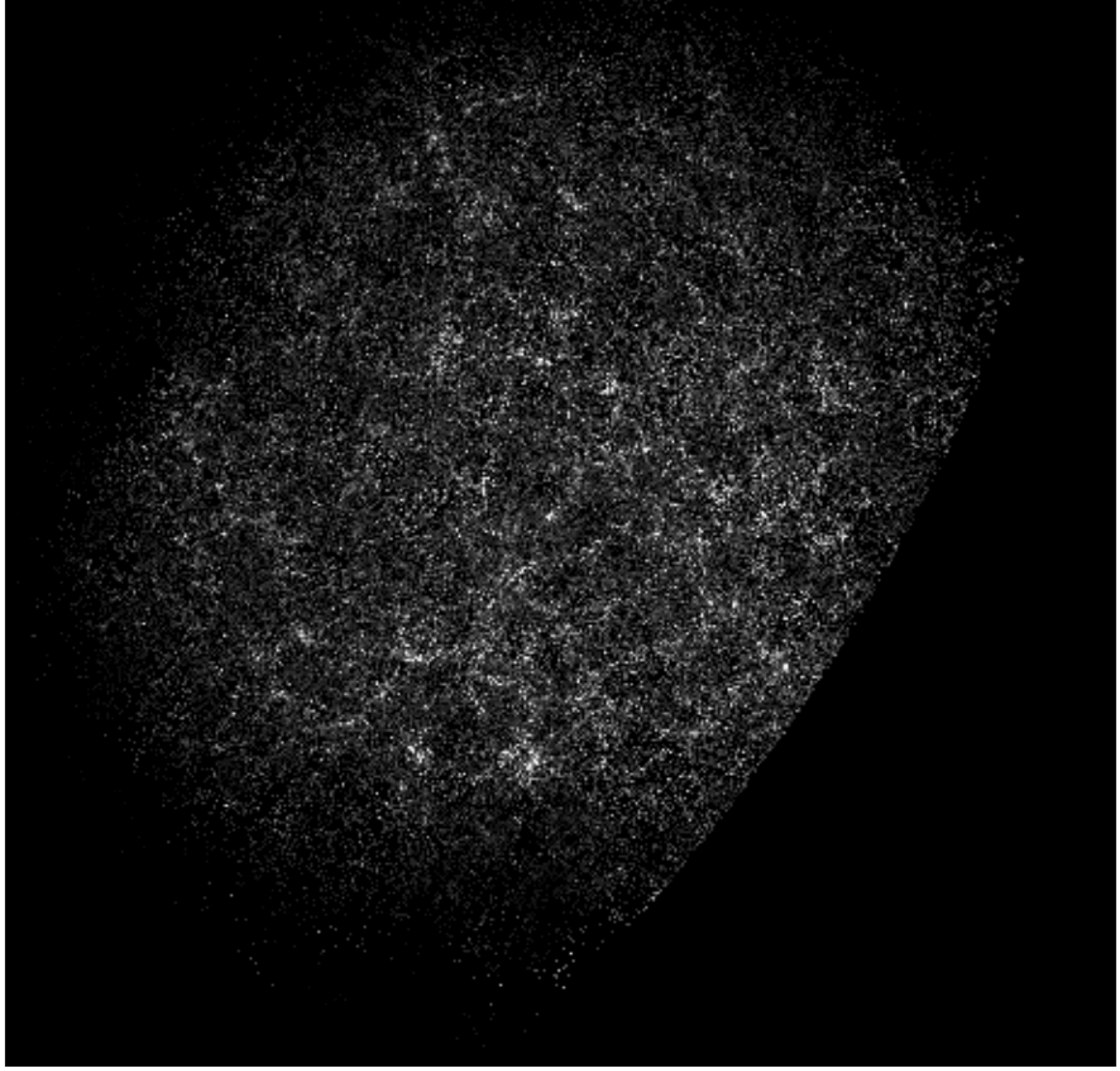

Fig. 6.1. The distribution of galaxies in the Northern sky, as compiled in the Lick catalog. This catalog contains the galaxy number counts for "pixels" of $10' \times 10'$ each. It is clearly seen that the distribution of galaxies on the sphere is far from being homogeneous. Instead it is distinctly structured

Clusters of Galaxies

1: Clusters of galaxies are the most massive gravitationally bound structures in the Universe. Typical values for the mass are $M \gtrsim 3 \times 10^{14} M_\odot$ for massive clusters, whereas for groups $M \sim 3 \times 10^{13} M_\odot$ is characteristic, with the total mass range of groups and clusters extending over $10^{12} M_\odot \lesssim M \lesssim 10^{15} M_\odot$.

2: Originally, clusters of galaxies were characterized as such by the observed spatial concentration of galaxies. Today we know that, although the galaxies determine the optical appearance of a cluster, the mass contained in galaxies contributes only a small fraction to the total mass of a cluster. Through advances in X-ray astronomy, it was discovered that galaxy clusters are intense sources of X-ray radiation which is emitted by a hot gas ($T \sim 3 \times 10^7$ K) located between the galaxies. This intergalactic gas (*intracluster medium*, ICM) contains more baryons than the stars seen in the member galaxies. From the dynamics of galaxies, from the properties of the X-ray emission of the clusters, and from the gravitational lens effect we deduce the existence of dark matter in galaxy clusters, dominating the cluster mass like it does for galaxies.

3: Clusters of galaxies play a very important role in observational cosmology. They are the most massive bound and relaxed (i.e., in a state of approximate dynamical equilibrium) structures in the Universe, as mentioned before, and therefore mark the most prominent density peaks of the large-scale structure in the Universe. Their cosmological evolution is therefore directly related to the growth of cosmic structures. Due to their high galaxy density, clusters and groups are also ideal laboratories for studying interactions between galaxies and their effect on the galaxy population. For instance, the fact that elliptical galaxies are preferentially found in clusters indicates the impact of the local galaxy density on the morphology and evolution of galaxies.

The Local Group

The galaxy group of which the Milky Way is a member is called the *Local Group*. Within a distance of ~ 1 Mpc around our Galaxy, about 35 galaxies are currently known; they are listed in Table 6.1. A sketch of their spatial distribution is given in Fig. 6.4.

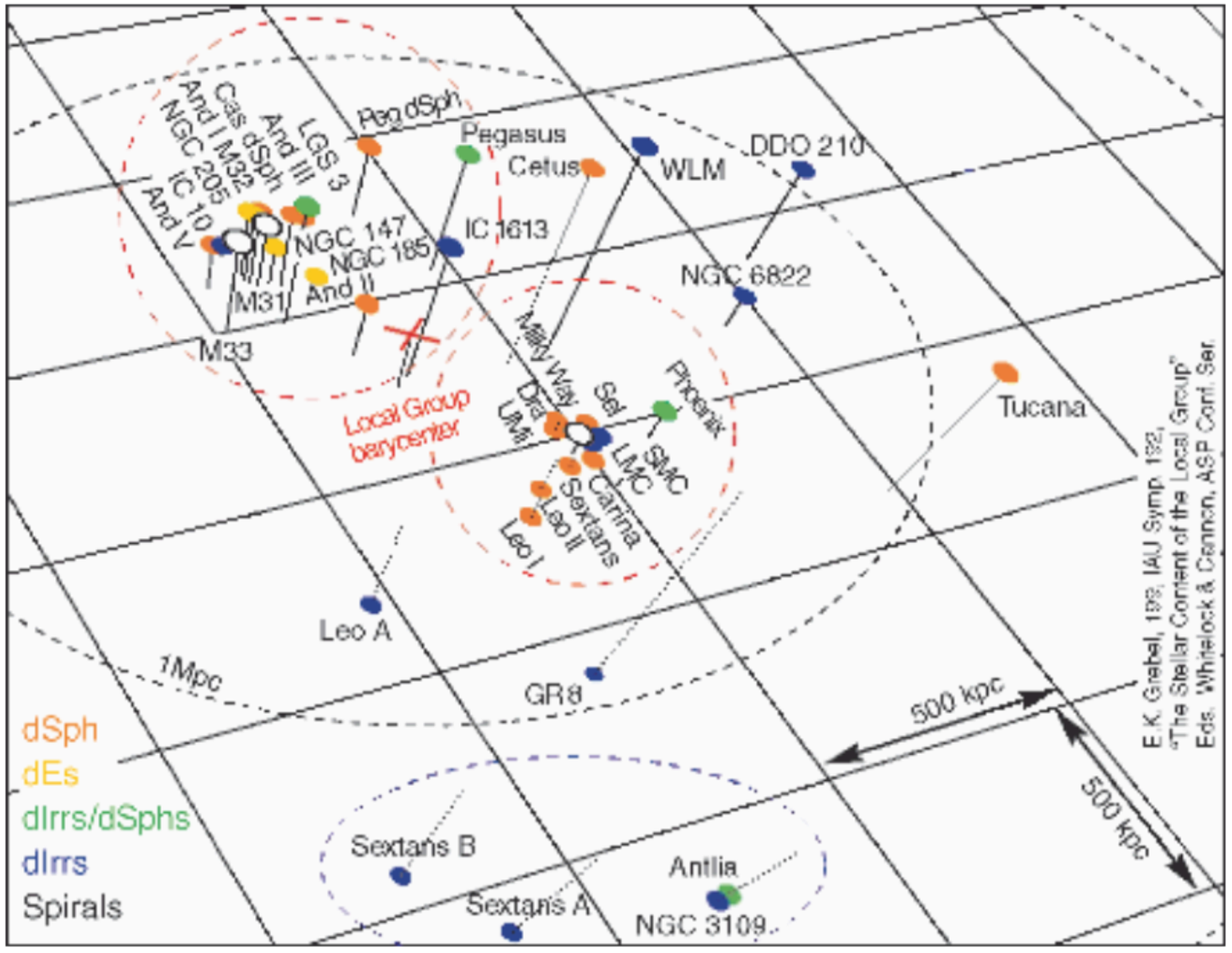

Fig. 6.4. Schematic distribution of galaxies in the Local Group, with the Milky Way at the center of the figure

Table 6.1. Members of the Local Group. Listed are the name of the galaxy, its morphological type, the absolute B-band magnitude, its position on the sphere in both right ascension/declination and in Galactic coordinates, its distance from the Sun, and its radial velocity. A sketch of the spatial configuration is displayed in Fig. 6.4

Galaxy	Type	M_B	RA/Dec.	ℓ, b	D (kpc)	v_r (km/s)
Milky Way	Sbc I-II	−20.0	1830 − 30	0, 0	8	0
LMC	Ir III-IV	−18.5	0524 − 60	280, −33	50	270
SMC	Ir IV-V	−17.1	0051 − 73	303, −44	63	163
Sgr I	dSph?		1856 − 30	6, −14	20	140
Fornax	dE0	−12.0	0237 − 34	237,−65	138	55
Sculptor Dwarf	dSph	−9.8	0057 − 33	286, −84	88	110
Leo I	dSph	−11.9	1005 + 12	226, +49	790	168
Leo II	dSph	−10.1	1110 + 22	220, +67	205	90
Ursa Minor	dSph	−8.9	1508 + 67	105, +45	69	−209
Draco	dSph	−9.4	1719 + 58	86, +35	79	−281
Carina	dSph	−9.4	0640 − 50	260, −22	94	229
Sextans	dSph	−9.5	1010 − 01	243, +42	86	230
M31	Sb I-II	−21.2	0040 + 41	121, −22	770	−297
M32=NGC 221	dE2	−16.5	0039 + 40	121, −22	730	−200
M110=NGC 205	dE5p	−16.4	0037 + 41	121, −21	730	−239
NGC 185	dE3p	−15.6	0036 + 48	121, −14	620	−202
NGC 147	dE5	−15.1	0030 + 48	120, −14	755	−193
And I	dSph	−11.8	0043 + 37	122, −25	790	—
And II	dSph	−11.8	0113 + 33	129, −29	680	—
And III	dSph	−10.2	0032 + 36	119, −26	760	—
Cas = And VII	dSph		2326 + 50	109, −09	690	—
Peg = DDO 216	dIr/dSph	−12.9	2328 + 14	94, −43	760	—
Peg II = And VI	dSph	−11.3	2351 + 24	106, −36	775	—
LGS 3	dIr/dSph	−9.8	0101 + 21	126, −41	620	−277
M33	Sc II-III	−18.9	0131 + 30	134, −31	850	−179
NGC 6822	dIr IV-V	−16.0	1942 − 15	025, −18	500	−57
IC 1613	dIr V	−15.3	0102 + 01	130, −60	715	−234
Sagittarius	dIr V	−12.0	1927 − 17	21, +16	1060	−79
WLM	dIr IV-V	−14.4	2359 − 15	76, −74	945	−116
IC 10	dIr IV	−16.0	0017 + 59	119, −03	660	−344
DDO 210, Aqr	dIr/dSph	−10.9	2044 − 13	34, −31	950	−137
Phoenix Dwarf	dIr/dSph	−9.8	0149 − 44	272, 68	405	56
Tucana	dSph	−9.6	2241 − 64	323, −48	870	—
Leo A = DDO 69	dIr V	−11.7	0959 + 30	196, 52	800	—
Cetus Dwarf	dSph	−10.1	0026 − 11	101, −72	775	—

1:

The Milky Way (MW), M31 (Andromeda), and M33 are the three spiral galaxies in the Local Group, and they are also its most luminous members. The Andromeda galaxy is located at a distance of 770 kpc from us. The Local Group member next in luminosity is the Large Magellanic Cloud (LMC, see Fig. 6.5), which is orbiting around the Milky Way, together with the Small Magellanic Cloud (SMC), at a distance of ~ 50 kpc (~ 60 kpc, respectively, for the SMC). Both are satellite galaxies of the Milky Way and belong to the class of irregular galaxies (like about 11 other Local Group members).

2:

The other members of the Local Group are dwarf galaxies, which are very small and faint. Because of their low luminosity and their low surface brightness, many of the known members of the Local Group have been detected only in recent years. For example, the Antlia galaxy, a dwarf spheroidal galaxy, was found in 1997. Its luminosity is about 10^4 times smaller than that of the Milky Way.

3: Many of the dwarf galaxies are grouped around the Galaxy or around M31; these are known as *satellite galaxies*. Distributed around the Milky Way are the LMC, the SMC, and nine dwarf galaxies, several of them in the so-called *Magellanic Stream* (see Fig. 6.6), a long, extended band of neutral hydrogen which was stripped from the Magellanic Clouds about 2×10^8 yr ago by tidal interactions with the Milky Way. The Magellanic Stream contains about $2 \times 10^8 M_\odot$ of neutral hydrogen.

4:

The spatial distribution of satellite galaxies around the Milky Way shows a pronounced peculiarity, in that these 11 satellites form a highly flattened system. These satellites appear to lie essentially in a plane which is oriented perpendicular to the Galactic plane. The satellites around M31 also seem to be distributed in an anisotropic way around their host. In fact, satellites galaxies around spirals seem to be preferentially located near the short axes of the projected light distribution, which has been termed the Holmberg effect, although the statistical significance of this alignment has been questioned.

The Local Group

Fig. 6.5. An image of the Large Magellanic Cloud (LMC), taken with the CTIO 4-m telescope

LMC & Magellanic Stream

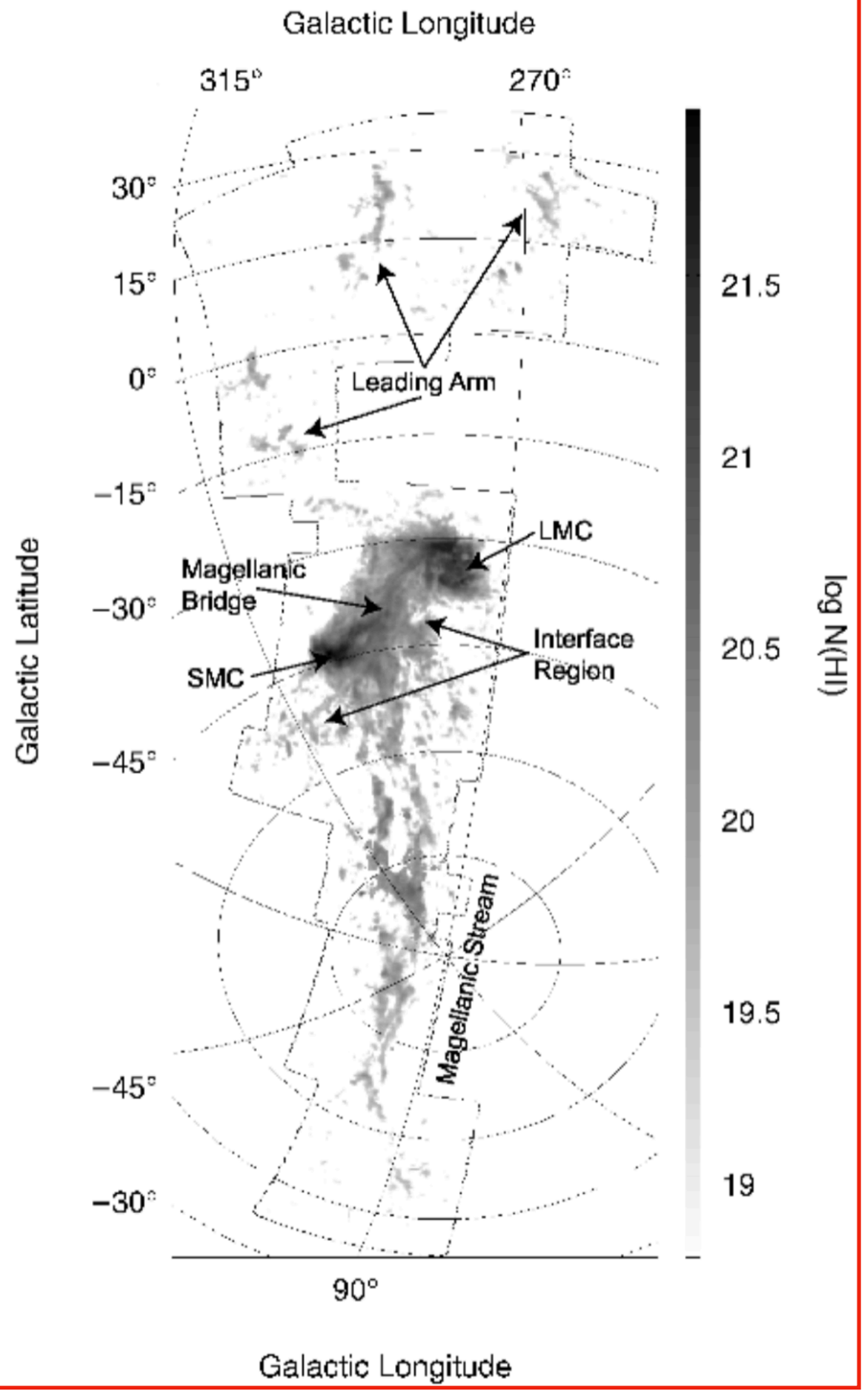

Fig. 6.6. HI map of a large region in the sky containing the Magellanic Clouds. This map is part of a large survey of HI, observed through its 21-cm line emission, that was performed with the Parkes telescope in Australia, and which maps about a quarter of the Southern sky with a pixel size of 5′ and a velocity resolution of $\sim$ 1 km/s. The emission from gas at Galactic velocities has been removed in this map. Besides the HI emission by the Magellanic Clouds themselves, gas between them is visible, the Magellanic Bridge and the Magellanic Stream, the latter connected to the Magellanic Clouds by an "interface region". Gas is also found in the direction of the orbital motion of the Magellanic Clouds around the Milky Way, forming the "leading arm"

The Mass of the Local Group

M31 is one of the very few galaxies with a blueshifted spectrum. Hence, Andromeda and the Milky Way are approaching each other at a relative velocity of $v \approx 120\,\mathrm{km/s}$. This value results from the velocity of M31 relative to the Sun of $v \approx 300\,\mathrm{km/s}$, and from the motion of the Sun around the Galactic center. Together with the distance to M31 of $D \sim 770\,\mathrm{kpc}$, we conclude that both galaxies will collide on a time-scale of $\sim 6 \times 10^9\,\mathrm{yr}$ (if we disregard the transverse component of the relative velocity).

The luminosity of the Local Group is dominated by the Milky Way and by M31, which together produce about 90% of the total luminosity. If the mass density follows the light distribution, the dynamics of the Local Group should also be dominated by these two galaxies. Therefore, one can try to estimate the mass of the two galaxies from their relative motion, and with this also the mass of the Local Group.

The Mass of the Local Group

In the early phases of the Universe, the Galaxy and M31 were close together and both took part in the Hubble expansion. By their mutual gravitational attraction, their relative motion was decelerated until it came to a halt – at a time $t_{\max}$ at which the two galaxies had their maximum separation $r_{\max}$ from each other. From this time on, they have been moving towards each other. The relative velocity $v(t)$ and the separation $r(t)$ follow from the conservation of energy,

$$\frac{v^2}{2} = \frac{GM}{r} - C\,, \tag{6.1}$$

where M is the sum of the masses of the Milky Way and M31 , and C is an integration constant. The latter can be determined by considering (6.1) at the time of maximum separation, when $r = r_{\max}$ and $v = 0$. With this,

$$C = \frac{GM}{r_{\max}}$$

follows immediately. Since $v = \mathrm{d}r/\mathrm{d}t$, (6.1) is a differential equation for $r(t)$,

$$\frac{1}{2}\left(\frac{\mathrm{d}r}{\mathrm{d}t}\right)^2 = GM\left(\frac{1}{r} - \frac{1}{r_{\max}}\right)\,.$$

It can be solved using the initial condition $r = 0$ at $t = 0$. For our purpose, an approximate consideration is sufficient. Solving the equation for $\mathrm{d}t$ we obtain, by integration, a relation between $r_{\max}$ and $t_{\max}$,

$$\begin{aligned} t_{\max} &= \int_0^{t_{\max}} \mathrm{d}t = \int_0^{r_{\max}} \frac{\mathrm{d}r}{\sqrt{2GM}\sqrt{1/r - 1/r_{\max}}} \\ &= \frac{\pi\, r_{\max}^{3/2}}{2\sqrt{2GM}}\,. \end{aligned} \tag{6.2}$$

Since the differential equation is symmetric with respect to changing $v \to -v$, the collision will happen at $2t_{\max}$. Estimating the time from today to the collision, by assuming the relative velocity to be constant during this time, then yields $r(t_0)/v(t_0) = D/v = 770\,\mathrm{kpc}/120\,\mathrm{km/s}$, and one obtains $2t_{\max} \approx t_0 + D/v$, or

$$t_{\max} \approx \frac{t_0}{2} + \frac{D}{2v}\,, \tag{6.3}$$

where t_0 is the current age of the Universe. Hence, together with (6.2) this yields

$$\frac{v^2}{2} = \frac{GM}{r} - \frac{GM}{r_{\max}} = \frac{GM}{r} - \frac{1}{2}\left(\frac{\pi GM}{t_{\max}}\right)^{2/3}\,. \tag{6.4}$$

The Mass of the Local Group

Now by inserting the values $r(t_0) = D$ and $v = v(t_0)$, we obtain the mass M,

$$M \sim 3 \times 10^{12} M_\odot \,, \tag{6.5}$$

where we have assumed $t_0 \approx 14 \times 10^9$ yr. This mass is much larger than the mass of the two galaxies as observed in stars and gas. The mass estimate yields a mass-to-light ratio for the Local Group of $M/L \sim 70\, M_\odot/L_\odot$. This is therefore another indication of the presence of dark matter because we can see only about 5% of the estimated mass in the Milky Way and Andromeda. Another mass estimate follows from the kinematics of the Magellanic Stream, which also yields $M/L \gtrsim 80 M_\odot/L_\odot$.

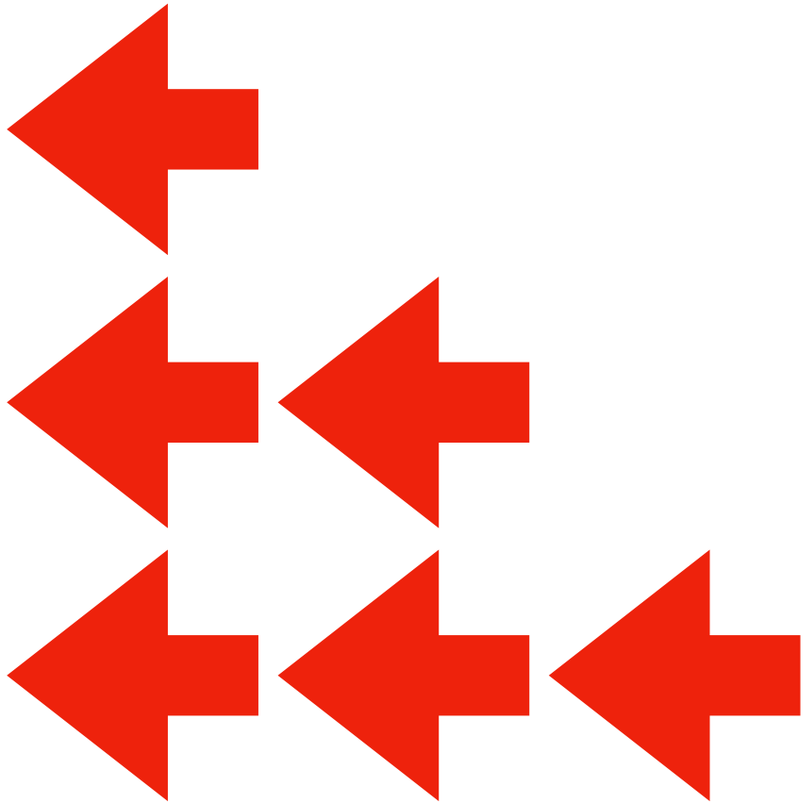

We see only 5% of mass in the Local Group => Dark Matter Dominated

Other components of the Local Group

One of the most interesting galaxies in the Local Group is the *Sagittarius dwarf galaxy* which was only discovered in 1994. Since it is located in the direction of the Galactic bulge, it is barely visible on optical images, if at all, as an overdensity of stars. Furthermore, it has a very low surface brightness. It was discovered in an analysis of stellar kinematics in the direction of the bulge, in which a coherent group of stars was found with a velocity distinctly different from that of bulge stars. In addition, the stars belonging to this overdensity have a much lower metallicity, reflected in their colors. The Sagittarius dwarf galaxy is located close to the Galactic plane, at a distance of about 16 kpc from the Galactic center and nearly in the direct extension of our line-of-sight to the GC. This proximity implies that it must be experiencing strong tidal gravitational forces on its orbit around the Milky Way; over the course of time, these will have the effect that the Sagittarius dwarf galaxy will be slowly disrupted. In fact, in recent years a relatively narrow band of stars has been found around the Milky Way. These stars are located along the orbit of the Sagittarius galaxy. Their chemical composition supports the interpretation that they are stars stripped from the Sagittarius dwarf galaxy by tidal forces. In addition, globular clusters have been identified which presumably once belonged to the Sagittarius dwarf galaxy, but which have also been removed from it by tidal forces and are now part of the globular cluster population in the Galactic halo.

Sagittarius Dwarf Irregular Galaxy (SDIG)

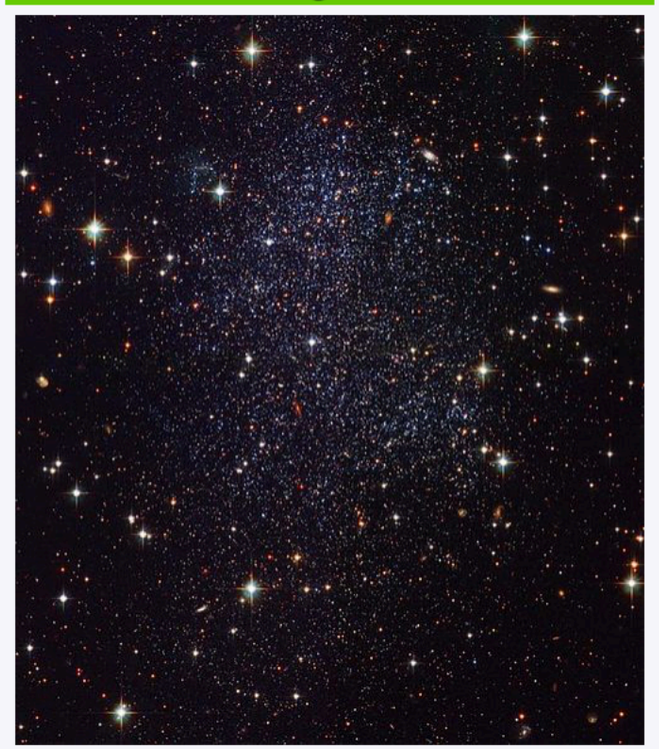

SagDIG by Hubble Space Telescope

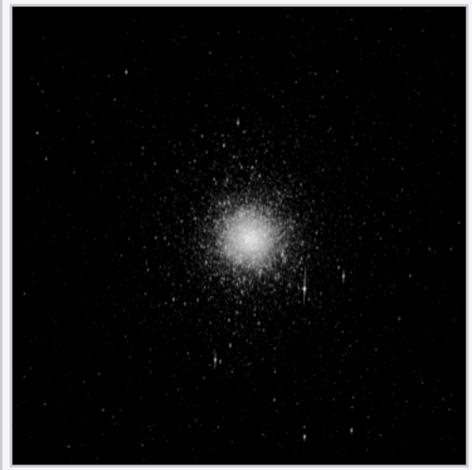
Messier 54, believed to be at the core of Sgr dSph. Greyscale image created from the HST's Advanced Camera for Surveys


Palomar 12, believed to have been captured from the Sgr dSph about 1.7 Gya

Other components of the Local Group

An all-sky map of high-velocity clouds

The distribution of HVCs

High-velocity clouds are not homogeneously distributed across the sky. Instead, they form large complexes, some of which extend over tens of degrees. The most famous and extended complexes in the northern hemisphere are complex A, C, and M, the first two of which were among the first HVCs ever detected in H I emission by Muller, Oort, and Raimond (1963) with the 25-m radio telescope near Dwingeloo. The southern hemisphere is dominated by the H I emission of the Magellanic Clouds, the Magellanic Stream, and the Leading Arm.

In addition to these large and prominent HVC complexes there are numerous compact HVCs all across the sky. Some of them have been grouped into complexes, including complex L, the complexes in the direction of the Galactic centre (GCP and GCN), or the so-called Wannier clouds (WA–WE). Other compact HVCs are completely isolated from any of the known complexes (e.g., Braun & Burton 1999), and their distances and origin are not well constrained.

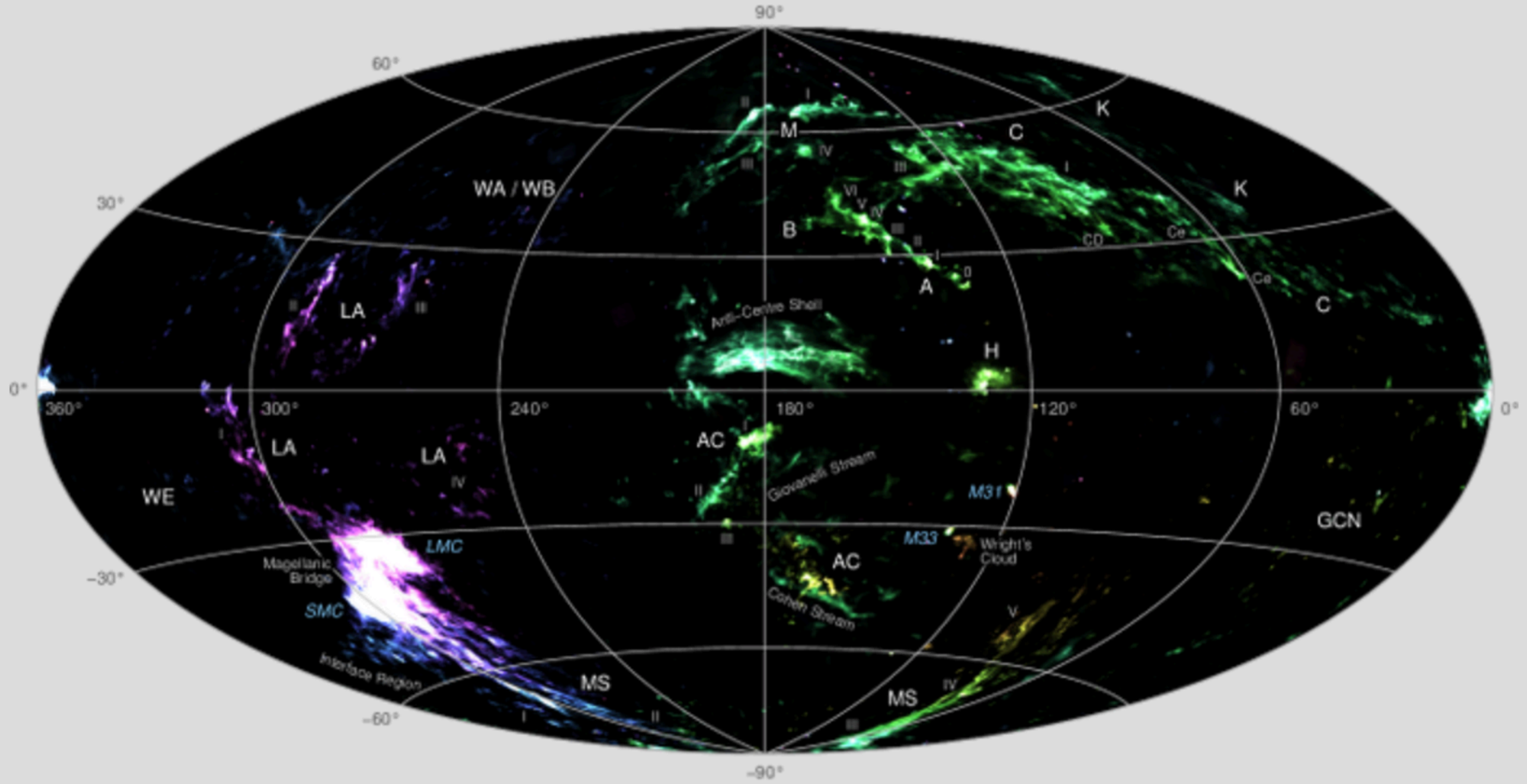

Fig. 1: All-sky false-colour map of high-velocity clouds. Intensity corresponds to H I column density in the range of 0 (black) to 10^{20} cm^{-2} (white), while hue represents LSR radial velocity in the range of –480 (red) to +480 kms^{-1} (purple).

Compact High Velocity Clouds

Compact high-velocity clouds (CHVCs) are high-velocity clouds (see Sect. 2.3.6) with an angular diameter of $\lesssim 1°$. The distance of these clouds is difficult to determine, since they do not seem to contain any stars, and hence the methods of distance determination based on stellar properties cannot be applied. In those cases where the spectrum of a background object shows an absorption line at the same radial velocity as determined for the cloud from measurements of the 21-cm line, an upper limit for the cloud distance is obtained; namely the distance of the object whose spectrum displays the absorption line.

Indirect arguments sometimes yield rather large estimates, of several hundred kpc, for the distance of the CHVCs. If their distance is indeed this large, the rotation curves of CHVCs, i.e., their differential infall velocities, suggest high masses for the clouds. In this model, CHVCs would contain a large fraction of dark matter, $M \sim 10^7 M_\odot$, and hence much more dark matter than their neutral hydrogen mass. CHVCs would then be additional members of the Local Group, having a mass not very different from that of dwarf galaxies, but in which star formation was suppressed for some reason so that they contain no, or only very few, stars.

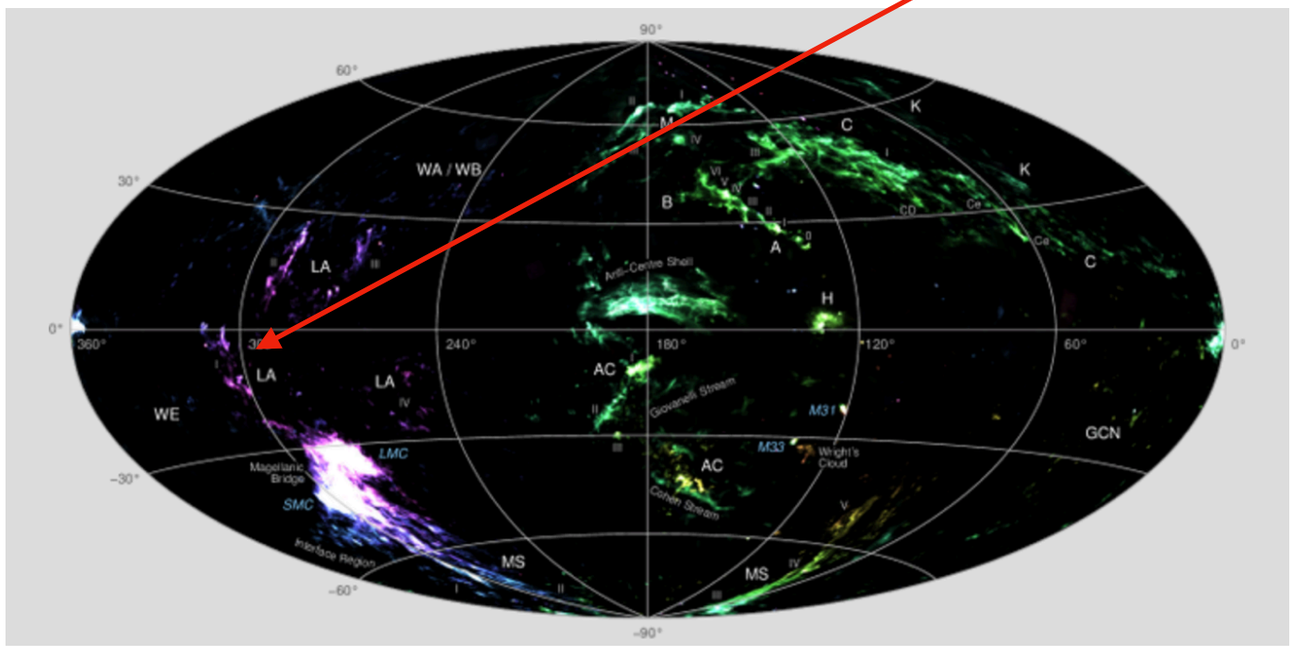

This model of CHVCs is controversial, however, and its verification or falsification would be of considerable interest for cosmology, as we will discuss later. If a concentration of CHVCs exists around the Milky Way at distances like the ones assumed in this model, a similar concentration should also exist around our sister galaxy M31. Currently, an intensive search for these systems is in progress. While HVCs have been found around M31, the search for CHVCs has been without success thus far. Therefore, one concludes a relatively low characteristic Galacto-centric distance for Galactic CHVCs of ~ 50 kpc. In this case, they would not be high-mass objects.

The neighborhood of the Local Group

The Neighborhood of the Local Group. The Local Group is indeed a concentration of galaxies: while it contains about 35 members within ~ 1 Mpc, the next neighboring galaxies are found only in the Sculptor Group, which contains about six members and is located at a distance of $D \sim 1.8$ Mpc. The next galaxy group after this is the M81 group of about eight galaxies at $D \sim 3.1$ Mpc, the two most prominent galaxies of which are displayed in Fig. 6.7.

Local Group (> 35 gal) within ~ 1 Mpc

Our closest neighbors:

Sculptor Group (6 gal) at ~ 1.8 Mpc

M81 Group (2 gal) at ~ 3.1 Mpc

Centaurus Group (17 gal) at ~ 3.5 Mpc

M101 Group (5 gal) at ~ 7.7 Mpc

M66 + M96 Group (10 gal) at ~ 9.4 Mpc

NGC 1023 Group (6 gal) at ~ 9.6 Mpc

Remember : $1 \text{ Mpc} = 3.086 \times 10^{24} \text{ cm}$

The other nearby associations of galaxies within 10 Mpc from us shall also be mentioned: the Centaurus group with 17 members and $D \sim 3.5$ Mpc, the M101 group with five members and $D \sim 7.7$ Mpc, the M66 and M96 group with together 10 members located at $D \sim 9.4$ Mpc, and the NGC 1023 group with six members at $D = 9.6$ Mpc. The numbers given here are those of currently known galaxies. Dwarf galaxies like Sagittarius would be very difficult to detect at the distances of these groups.

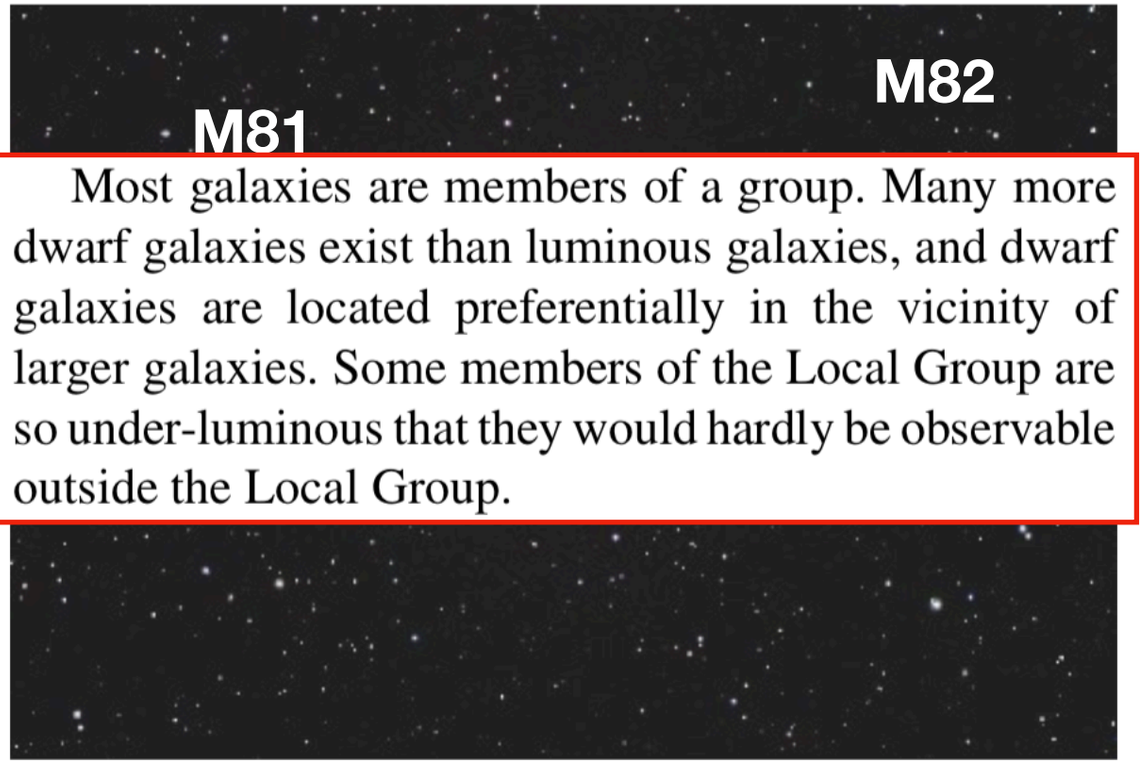

Most galaxies are members of a group. Many more dwarf galaxies exist than luminous galaxies, and dwarf galaxies are located preferentially in the vicinity of larger galaxies. Some members of the Local Group are so under-luminous that they would hardly be observable outside the Local Group.

Fig. 6.7. M81 (left) and M82 (right), two galaxies of the M81 group, about 3.1 Mpc away. These two galaxies are moving around each other, and the gravitational interaction taking place may be the reason for the violent star formation in M82. M82 is an archetypical starburst galaxy

Clusters of galaxies

One large concentration of galaxies was already known in the eighteenth century (W. Herschel) – the *Virgo Cluster*. Its galaxies extend over a region of about $10° \times 10°$ in the sky, and its distance is $D \sim 16$ Mpc. The Virgo Cluster consists of about 250 large galaxies and more than 2000 smaller ones. In the classification scheme of galaxy clusters, Virgo is considered an irregular cluster. The closest regular massive galaxy cluster is the *Coma cluster* (see Fig. 1.14), at a distance of about $D \sim 90$ Mpc.

Coma Cluster, > 1000 lum gal, at ~ 90 Mpc —>

Fig. 1.14. The Coma cluster of galaxies, at a distance of roughly 90 Mpc from us, is the closest massive regular cluster of galaxies. Almost all objects visible in this image are galaxies associated with the cluster – Coma contains more than a thousand luminous galaxies

<— Virgo Cluster, > 250 lum gal, at ~ 16 Mpc

Clusters of galaxies

6.2.1 The Abell Catalog

George Abell compiled a catalog of galaxy clusters, published in 1958, in which he identified regions in the sky that show an overdensity of galaxies. This identification was performed by eye on photoplates from the *Palomar Observatory Sky Survey* (POSS), a photographic atlas of the Northern ($\delta > -30°$) sky.[1] He omitted the Galactic disk region because the observation of galaxies is considerably more problematic there, due to extinction and the high stellar density (see also Fig. 6.2).

Coma Cluster =
Abell 1656
z= 0.0231

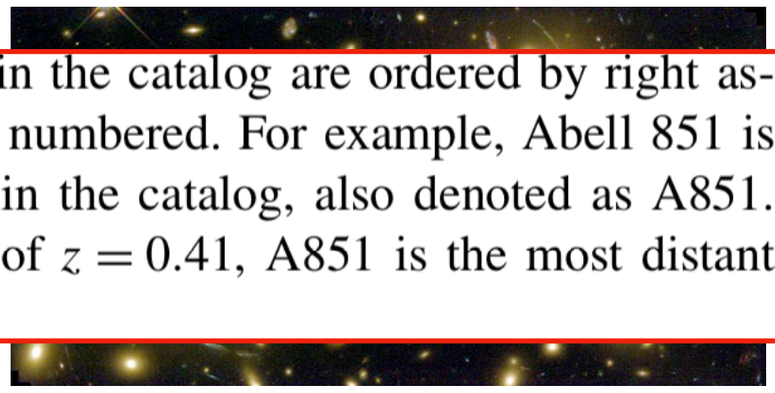

Abell 2218

The clusters in the catalog are ordered by right ascension and are numbered. For example, Abell 851 is the 851st entry in the catalog, also denoted as A851. With a redshift of $z = 0.41$, A851 is the most distant Abell cluster.

Abell's Criteria and his Catalog. The criteria Abell applied for the identification of clusters refer to an overdensity of galaxies within a specified solid angle. According to these criteria, a cluster contains ≥ 50 galaxies in a magnitude interval $m_3 \leq m \leq m_3 + 2$, where m_3 is the apparent magnitude of the third brightest galaxy in the cluster.[2] These galaxies must be located within a circle of angular radius

$$\theta_A = \frac{1.'7}{z} \tag{6.6}$$

where z is the estimated redshift. The latter is determined by the assumption that the luminosity of the tenth brightest galaxy in a cluster is the same for all clusters. A calibration of this distance estimate is performed on clusters of known redshift. θ_A is called the *Abell radius* of a cluster, and corresponds to a physical radius of $R_A \approx 1.5 h^{-1}$ Mpc.

The Abell catalog contains 1682 clusters which all fulfill the above criteria. In addition, it lists 1030 clusters that have been found in the search, but which do not fulfill all of the criteria (most of these contain between 30 and 49 galaxies). An extension of the catalog to the Southern sky was published by Abell, Corwin & Olowin in 1989. This ACO catalog contains 4076 clusters, including the members of the original catalog. Another important catalog of galaxy clusters is the Zwicky catalog (1961–68), which contains more clusters, but for which the applied selection criteria are considered less reliable.

[1]

Clusters of galaxies

Abell Classes. The Abell and ACO catalogs divide clusters into so-called richness and distance classes. Table 6.2 lists the criteria for the richness classes, while Table 6.3 lists those for the distance classes.

There are six *richness classes*, denoted from 0 to 5, according to the number of cluster member galaxies. Richness class 0 contains between 30 and 49 members and therefore does not belong to the cluster catalog proper. One can see from Table 6.2 that the number of clusters rapidly decreases with increasing richness class, so only very few clusters exist with a very large number of cluster galaxies. As a reminder, the region of the sky from where the Abell clusters were detected is about 2/3 of the total sphere. Thus, only a few very rich clusters do indeed exist (at redshift $\lesssim 0.2$).

The subdivision into six *distance classes* is based on the apparent magnitude of the tenth brightest galaxy, in accordance with the redshift estimate for the cluster. Hence, the distance class provides a coarse measure of the distance.

Table 6.2. Definition of Abell's richness classes. N is the number of cluster galaxies with magnitudes between m_3 and $m_3 + 2$ inside the Abell radius (6.6), where m_3 is the brightness of the third brightest cluster galaxy.

Richness class R	N	Number in Abell's catalog
(0)	(30–49)	(≥ 1000)
1	50–79	1224
2	80–129	383
3	130–199	68
4	200–299	6
5	≥ 300	1

Table 6.3. Definition of Abell's distance classes. m_{10} is the magnitude of the tenth brightest cluster galaxy.

Distance class	m_{10}	Estimated average redshift	Number in Abell's catalog with $R \geq 1$
1	13.3–14.0	0.0283	9
2	14.1–14.8	0.0400	2
3	14.9–15.6	0.0577	33
4	15.7–16.4	0.0787	60
5	16.5–17.2	0.131	657
6	17.3–18.0	0.198	921

Clusters of galaxies

6.2.2 Luminosity Function of Cluster Galaxies

The luminosity function of galaxies in a cluster is defined as in Sect. 3.7 for the total galaxy population. In many clusters, the Schechter luminosity function (3.38) represents a very good fit to the data if the brightest galaxy is disregarded in each cluster (see Fig. 3.32 for the Virgo Cluster of galaxies). The slope α at the faint end is not easy to determine, since projection effects become increasingly important for fainter galaxies. The value of α seems to vary between clusters, but it is not entirely clear whether this result may also be affected by projection effects in different clusters of differing strength. Thus, no final conclusion has been reached as to whether the luminosity function has a steep increase at $L \ll L^*$ or not, i.e., whether many more faint galaxies exist than luminous $\sim L^*$-galaxies (compare the galaxy content in the Local Group, Sect. 6.1.1, where even in our close neighborhood it is difficult to obtain a complete census of the galaxy population). L^* is very similar for many clusters, which is the reason why the distance estimate by apparent brightness of cluster members is quite reliable. However, a number of clusters exists with a clearly deviating value of L^*.

- Schechter function OK for many clusters

- Slope α at the faint end not well defined

  - projection effects
  - contamination

- L^* very similar for many (not all) clusters

  - can be used as standard candle

- cD galaxies in the center of many clusters, where galaxy density is strongly enhanced

Many clusters contain *cD galaxies* at their centers; these differ from large ellipticals in several respects. They have a very extended stellar envelope, whose size may exceed $R \sim 100$ kpc and whose surface brightness profile is much broader than that of a de Vaucouleurs profile (see Fig. 3.8). cD galaxies are found only in the centers of clusters or groups, thus only in regions of strongly enhanced galaxy density. Many cD galaxies have multiple cores, which is a rather rare phenomenon among the other cluster members.

Clusters of galaxies

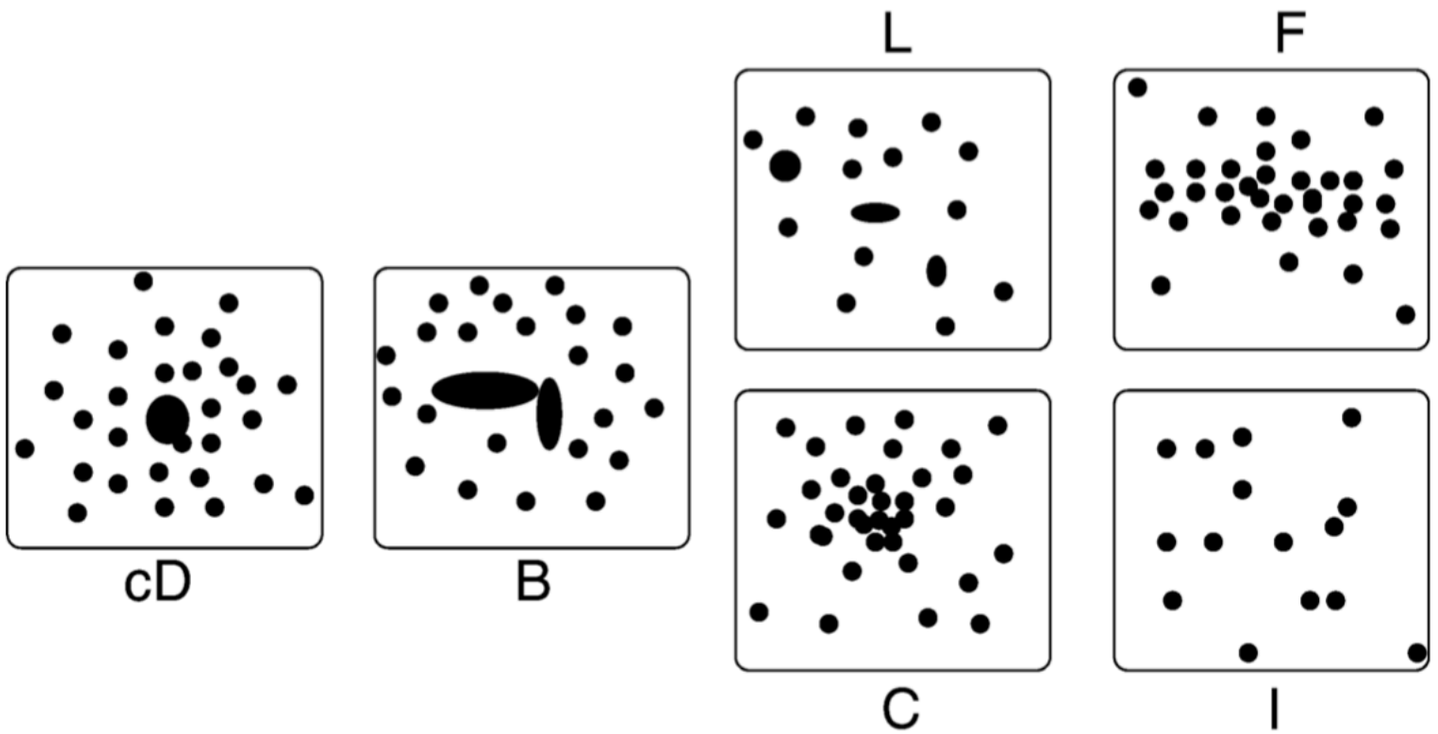

Fig. 6.8. Rough morphological classification of clusters by Rood & Sastry: cDs are those which are dominated by a central cD galaxy, Bs contain a pair of bright galaxies in the center. Ls are clusters with a nearly linear alignment of the dominant galaxies, Cs have a single core of galaxies, Fs are clusters with an oblate galaxy distribution, and Is are clusters with an irregular distribution

6.2.3 Morphological Classification of Clusters

Clusters are also classified by the morphology of their galaxy distribution. Several classifications are used, one of which is displayed in Fig. 6.8. Since this is a description of the visual impression of the galaxy distribution, the exact class of a cluster is not of great interest. However, a rough classification can provide an idea of the state of a cluster, i.e., whether it is currently in dynamical equilibrium or whether it has been heavily disturbed by a merger process with another cluster. Therefore, one distinguishes in particular between regular and irregular clusters, and also those which are intermediate; the transition between classes is of course continuous. Regular clusters are compact whereas, in contrast, irregular clusters are "open" (Zwicky's classification criteria).

This morphological classification indeed points at physical differences between clusters, as correlations between morphology and other properties of galaxy clusters show. For example, it is found that regular clusters are completely dominated by early-type galaxies, whereas irregular clusters have a fraction of spirals nearly as large as in the general distribution of field galaxies. Very often, regular clusters are dominated by a cD galaxy at the center, and their central galaxy density is very high. In contrast, irregular clusters are significantly less dense in the center. Irregular clusters often show strong substructure, which is rarely found in regular clusters. Furthermore, regular clusters have a high richness, whereas irregular clusters have fewer cluster members. To summarize, regular clusters can be said to be in a relaxed state, whereas irregular clusters are still in the process of evolution.

Clusters of galaxies

6.2.4 Spatial Distribution of Galaxies

Most regular clusters show a centrally condensed number density distribution of cluster galaxies, i.e., the galaxy density increases strongly towards the center. If the cluster is not very elliptical, this density distribution can be assumed, to a first approximation, as being spherically symmetric. Only the projected density distribution $N(R)$ is observable. This is related to the three-dimensional number density $n(r)$ through

$$N(R) = \int_{-\infty}^{\infty} \mathrm{d}z\, n\left(\sqrt{R^2+z^2}\right) = 2\int_{R}^{\infty} \frac{\mathrm{d}r\, r\, n(r)}{\sqrt{r^2-R^2}}\,, \tag{6.7}$$

where in the second step a simple transformation of the integration variable from the line-of-sight coordinate z to the three-dimensional radius $r = \sqrt{R^2+z^2}$ was made.

(density projected on the sky)

Consider parametrized form of $N(R)$ and fit the observed galaxy distribution

5 parameters needed to describe $N(R)$

- **position of cluster center (2 parameters)**
- **number of galaxies at cluster center $N(0)$**
- **characteristic scale r_c, where $N(r_c) = N_0/2$.**
- **cluster radius (where the cluster ends)**

For example, King Model:

$$\rho(r) = \rho_0 \left[1+\left(\frac{r}{r_c}\right)^2\right]^{-3/2} \qquad r_c \sim 0.25 h^{-1}\,\mathrm{Mpc}$$

$$\Sigma(R) = \Sigma_0 \left[1+\left(\frac{R}{r_c}\right)^2\right]^{-1} \quad \text{with} \quad \Sigma_0 = 2\rho_0 r_c$$

Clusters of galaxies

6.2.5 Dynamical Mass of Clusters

The above argument relates the velocity distribution of cluster galaxies to the mass profile of the cluster, and from this we obtain physical models for the density distribution. This implies the possibility of deriving the mass, or the mass profile, respectively, of a cluster from the observed velocities of cluster galaxies. We will briefly present this method of mass determination here. For this, we consider the dynamical time-scale of clusters, defined as the time a typical galaxy needs to traverse the cluster once,

$$\boxed{t_{\rm cross} \sim \frac{R_{\rm A}}{\sigma_v} \sim 1.5 h^{-1} \times 10^9\,{\rm yr}} \quad , \tag{6.18}$$

where a (one-dimensional) velocity dispersion $\sigma_v \sim 1000\,{\rm km/s}$ was assumed. The dynamical time-scale is shorter than the age of the Universe. One therefore concludes that clusters of galaxies are gravitationally bound systems. If this were not the case they would dissolve on a timescale $t_{\rm cross}$. Since $t_{\rm cross} \ll t_0$ one assumes a *virial equilibrium*, hence that the virial theorem applies, so that in a time-average sense,

$$2E_{\rm kin} + E_{\rm pot} = 0 \,, \tag{6.19}$$

where

$$E_{\rm kin} = \frac{1}{2}\sum_i m_i\, v_i^2 \,; \quad E_{\rm pot} = -\frac{1}{2}\sum_{i\neq j} \frac{G m_i m_j}{r_{ij}} \tag{6.20}$$

are the kinetic and the potential energy of the cluster galaxies, m_i is the mass of the i-th galaxy, v_i is the absolute value of its velocity, and r_{ij} is the spatial separation between the i-th and the j-th galaxy. The factor $1/2$ in the definition of $E_{\rm pot}$ occurs since each pair of galaxies occurs twice in the sum.

We define the total mass of the cluster,

$$M := \sum_i m_i \,, \tag{6.21}$$

the velocity dispersion, weighted by mass,

$$\langle v^2 \rangle := \frac{1}{M}\sum_i m_i\, v_i^2 \tag{6.22}$$

and the gravitational radius,

$$r_{\rm G} := 2M^2 \left(\sum_{i\neq j} \frac{m_i\, m_j}{r_{ij}} \right)^{-1} \,. \tag{6.23}$$

With this, we obtain

$$E_{\rm kin} = \frac{M}{2}\langle v^2 \rangle \,; \quad E_{\rm pot} = -\frac{G\,M^2}{r_{\rm G}} \,, \tag{6.24}$$

for the kinetic and potential energy. Applying the virial theorem (6.19) yields the mass estimate

$$\boxed{M = \frac{r_{\rm G}\langle v^2 \rangle}{G}} \,. \tag{6.25}$$

Clusters of galaxies

The "Missing Mass" Problem in Clusters of Galaxies. With M and the number N of galaxies, one can now derive a characteristic mass $m = M/N$ for the luminous galaxies. This mass is found to be very high, $m \sim 10^{13} M_\odot$. Alternatively, M can be compared with the total optical luminosity of the cluster galaxies, $L_{\rm tot} \sim 10^{12}$–$10^{13}\, L_\odot$, and hence the mass-to-light ratio can be calculated; typically

$$\left(\frac{M}{L_{\rm tot}}\right) \sim 300\, h \left(\frac{M_\odot}{L_\odot}\right) . \qquad (6.28)$$

This value exceeds the M/L ratio of early-type galaxies by at least a factor of 10. Realizing this discrepancy, Fritz Zwicky concluded as early as 1933, from an analysis of the Coma cluster, that clusters of galaxies must contain considerably more mass than is visible in galaxies – the dawn of the *missing mass problem*. As we will see further below, this problem has by now been firmly established, since other methods for the mass determination of clusters also yield comparable values and indicate that a major fraction of the mass in galaxy clusters consists of (non-baryonic) dark matter. *The stars visible in galaxies contribute less than about 5% to the total mass in clusters of galaxies.*

$$M = \frac{3\pi R_{\rm G} \sigma_v^2}{2G} = 1.1 \times 10^{15} M_\odot \left(\frac{\sigma_v}{1000\,{\rm km/s}}\right)^2 \left(\frac{R_{\rm G}}{1\,{\rm Mpc}}\right) . \qquad (6.27)$$

We explicitly point out that this mass estimate no longer depends on the masses m_i of the individual galaxies – rather the galaxies are now test particles in the gravitational potential. With $\sigma_v \sim 1000$ km/s and $R_{\rm G} \sim 1$ Mpc as typical values for rich clusters of galaxies, one obtains a characteristic mass of $\sim 10^{15} M_\odot$ for rich clusters.

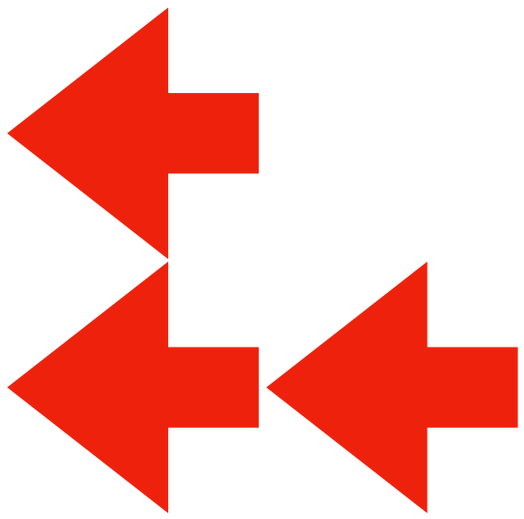

Clusters of galaxies

6.2.9 The Morphology–Density Relation

As mentioned several times before, the mixture of galaxy types in clusters differs from that of isolated (field) galaxies. Whereas about 70% of the field galaxies are spirals, clusters are dominated by early-type galaxies, in particular in their inner regions. Furthermore, the fraction of spirals in a cluster depends on the distance to the center and increases for larger r. Obviously, the local density has an effect on the morphological mix of galaxies.

vs. local density **vs. distance from cluster center**

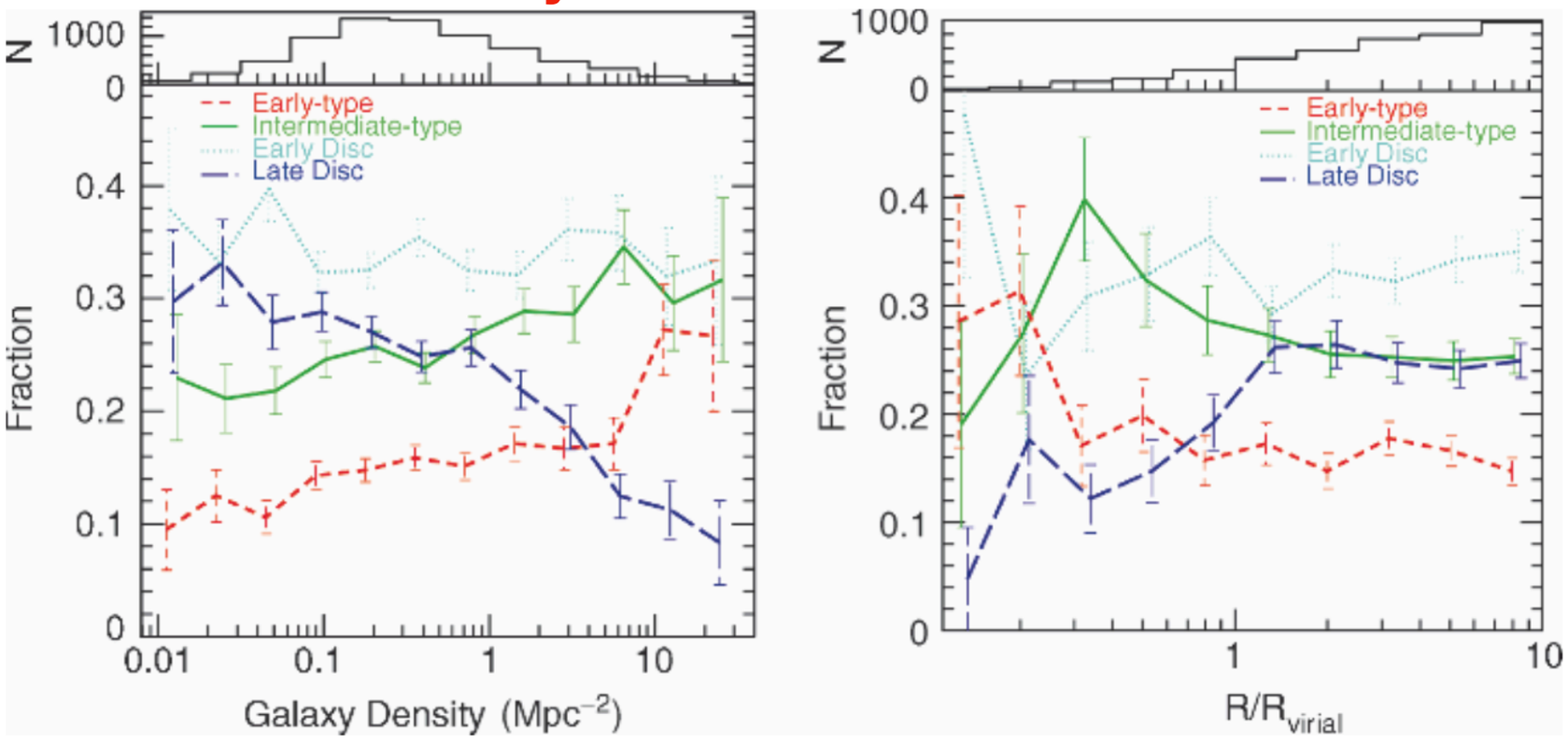

Fig. 6.11. The number fraction of galaxies of different morphologies is plotted as a function of the local galaxy density (left panel), and for galaxies in clusters as a function of the distance from the cluster center, scaled by the corresponding virial radius (right panel). Galaxies have been divided into four different classes. "Early-types" contain mainly ellipticals, "intermediates" are mainly S0 galaxies, "early and late disks" are predominantly Sa and Sc spirals, respectively. In both representations, a clear dependence of the galaxy mix on the density or on the distance from the cluster center, respectively, is visible. In the histograms at the top of each panel, the number of galaxies in the various bins is plotted

Clusters of galaxies

6.3 X-Ray Radiation from Clusters of Galaxies

One of the most important discoveries of the UHURU X-ray satellite, launched in 1970, was the detection of X-ray radiation from massive clusters of galaxies. With the later Einstein X-ray satellite and more recently ROSAT, X-ray emission was also detected from lower-mass clusters and groups. Three examples for the X-ray emission of galaxy clusters are displayed in Figs. 6.13–6.15. Figure 6.13 shows the Coma cluster of galaxies, observed with two different X-ray observatories. Although Coma was considered to be a fully relaxed cluster, distinct substructure is visible in its X-ray radiation. The cluster RXJ 1347−1145 (Fig. 6.14) is regarded as the most luminous cluster in the X-ray domain. A large mass estimate of this cluster also follows from the analysis of the gravitationally lensed arcs (see Sect. 6.5) that are visible in Fig. 6.14; the cover of this book shows a more recent image of this cluster, taken with the ACS camera on-board HST, where a large number of arcs can be readily detected. Finally, Fig. 6.15 shows a superposition of the X-ray emission and an optical image of the cluster MS 1054−03, which is situated at $z = 0.83$ and to which we will refer as an example frequently below.

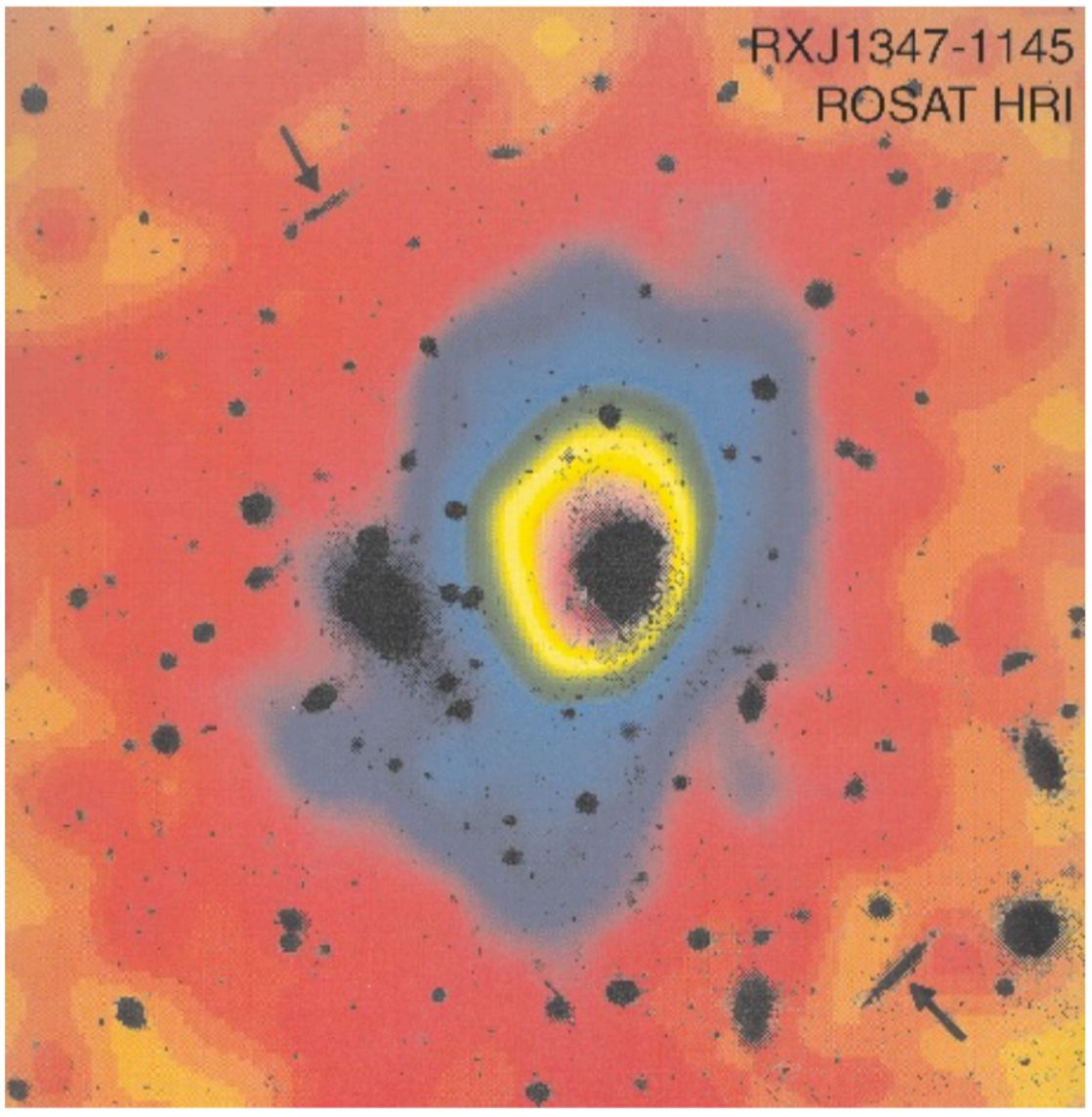

Fig. 6.14. RXJ 1347−1145 is the most luminous galaxy cluster in the X-ray domain. A color-coded ROSAT/HRI image of this cluster, which shows the distribution of the intergalactic gas, is superposed on an optical image of the cluster. The two arrows indicate giant arcs, images of background galaxies which are strongly distorted by the gravitational lens effect

6.3.1 General Properties of the X-Ray Radiation

Clusters of galaxies are the brightest extragalactic X-ray sources besides AGNs. Their characteristic luminosity is $L_X \sim 10^{43}$ up to $\sim 10^{45}$ erg/s for the most massive clusters. This X-ray emission from clusters is spatially extended, so it does not originate in individual galaxies. The spatial region from which we can detect this radiation can have a size of 1 Mpc or even larger. Furthermore, the X-ray radiation from clusters does not vary on timescales over which it has been observed ($\lesssim 30$ yr). Variations would also not be expected if the radiation originates from an extended region.

Continuum Radiation. The spectral energy distribution of the X-rays leads to the conclusion that the emission process is optically thin thermal bremsstrahlung (free–free radiation) from a hot gas. This radiation is produced by the acceleration of electrons in the Coulomb field of protons and atomic nuclei. Since an accelerated electrically charged particle emits radiation, such scattering processes between electrons and protons in an ionized gas yields emission of photons. From the spectral properties of this radiation, the gas temperature in galaxy clusters can be determined, which is, for clusters with mass between $\sim 10^{14} M_\odot$ and $\sim 10^{15} M_\odot$, in the range of 10^7–10^8 K, or 1–10 keV, respectively.

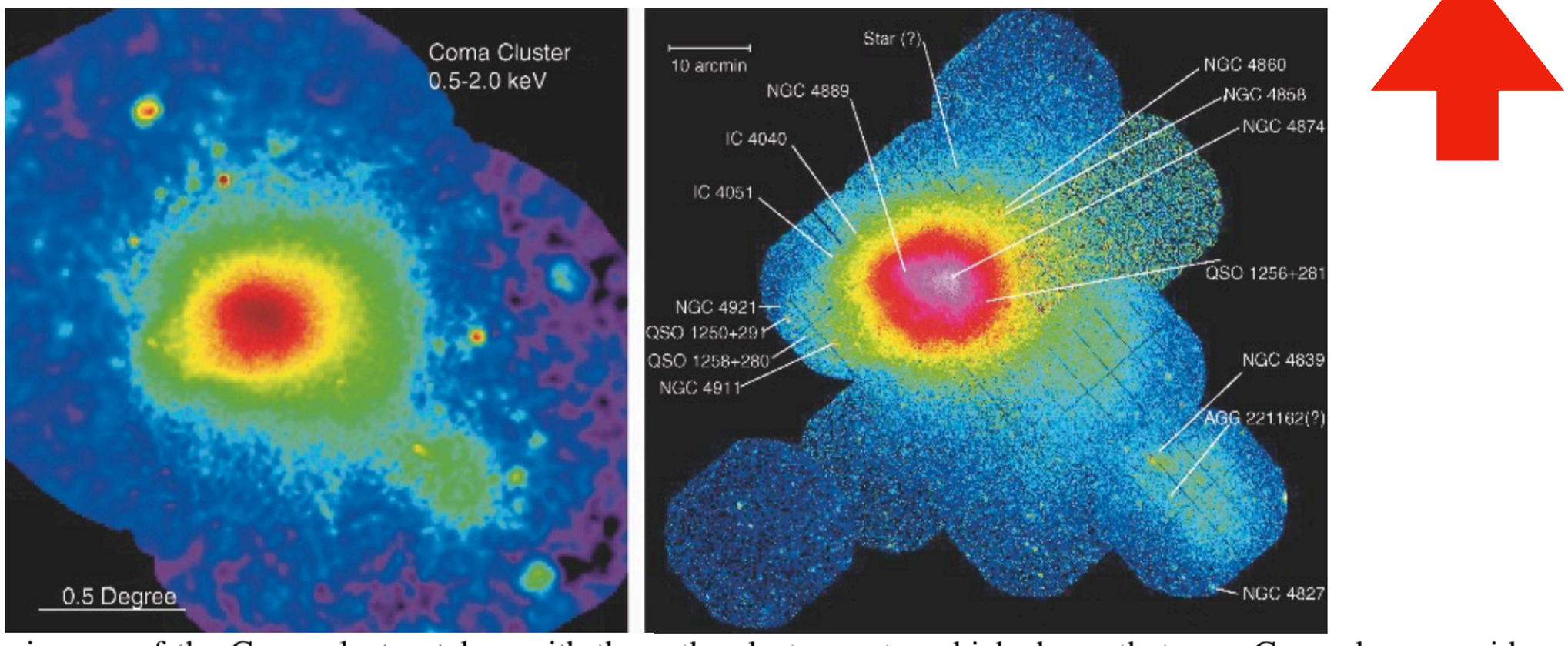

Fig. 6.13. X-ray images of the Coma cluster, taken with the ROSAT-PSPC (left) and XMM-EPIC (right). The image size in the left panel is $2.7° \times 2.5°$. A remarkable feature is the secondary maximum in the X-ray emission at the lower right of the cluster center which shows that even Coma, long considered to be a regular cluster, is not completely in an equilibrium state, but is dynamically evolving, presumably by the accretion of a galaxy group

Clusters of galaxies

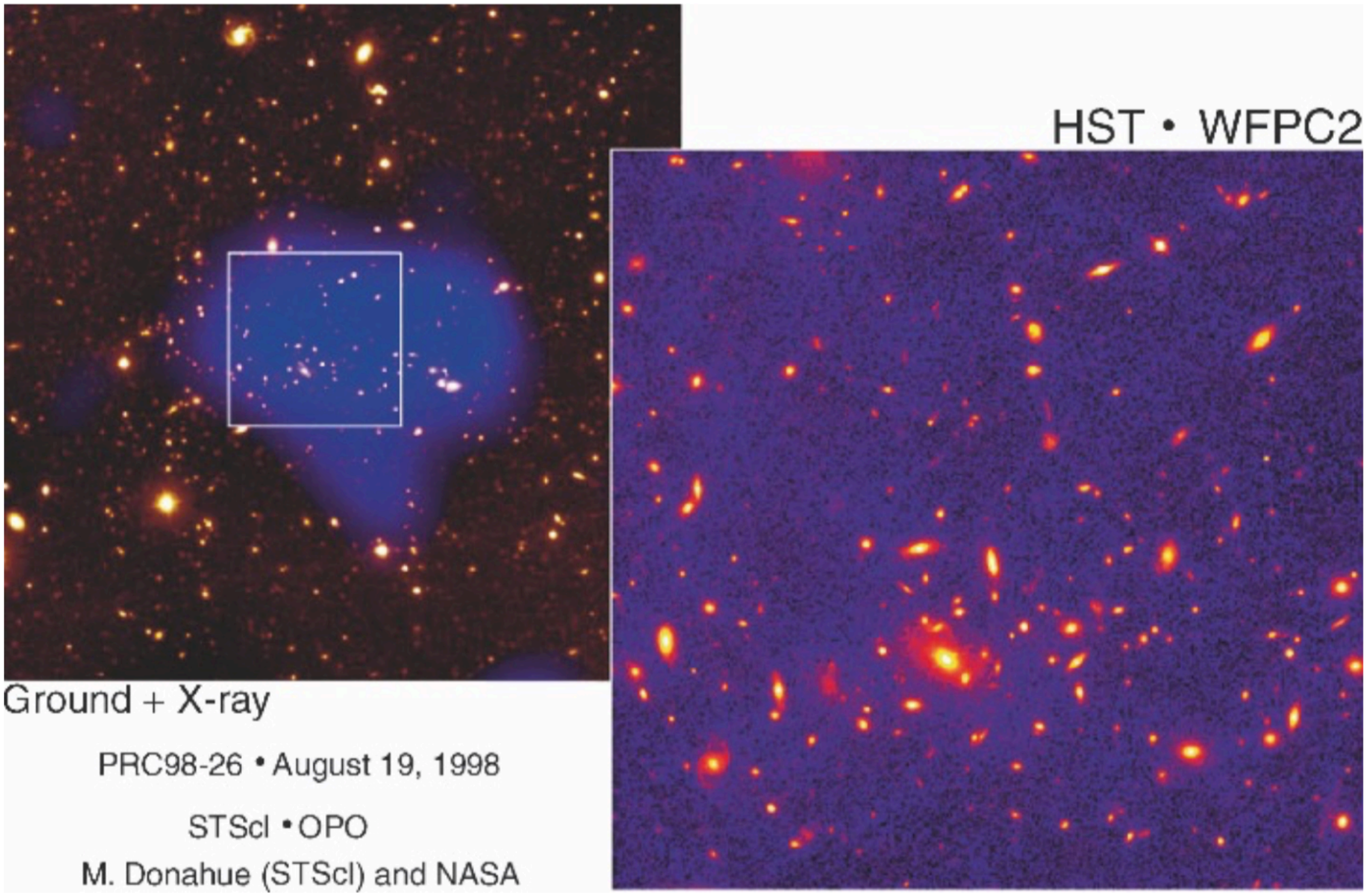

Fig. 6.15. The cluster of galaxies MS 1054−03 is, at $z = 0.83$, the highest-redshift cluster in the Einstein Medium Sensitivity Survey, which was compiled from observations with the Einstein satellite (see Sect. 6.3.5). On the right, an HST image of the cluster is shown, while on the left is an optical image, obtained with the 2.2-m telescope of the University of Hawaii, superposed (in blue) with the X-ray emission of the cluster measured with the ROSAT-HRI

Clusters of galaxies

6.5 Clusters of Galaxies as Gravitational Lenses

6.5.1 Luminous Arcs

In 1986, two groups independently discovered unusually stretched, arc-shaped sources in two clusters of galaxies at high redshift (see Figs. 6.30 and 6.31). The nature of these sources was unknown at first; they were named *arcs*, or *giant luminous arcs*, which did not imply any interpretation originally. Different hypotheses for the origin of these arcs were formulated, like for instance emission by shock fronts in the ICM, originating from explosive events. All these scenarios were disproven when the spectroscopy of the arc in the cluster Abell 370 showed that the source is at a much higher redshift than the cluster itself. Thus, the arc is a background source, subject to the gravitational lens effect (see Sect. 3.8) of the cluster. By differential light deflection, the light beam of the source can be distorted in such a way that highly elongated arc-shaped images are produced.

The discovery that clusters of galaxies may act as strong gravitational lenses came as a surprise at that time.

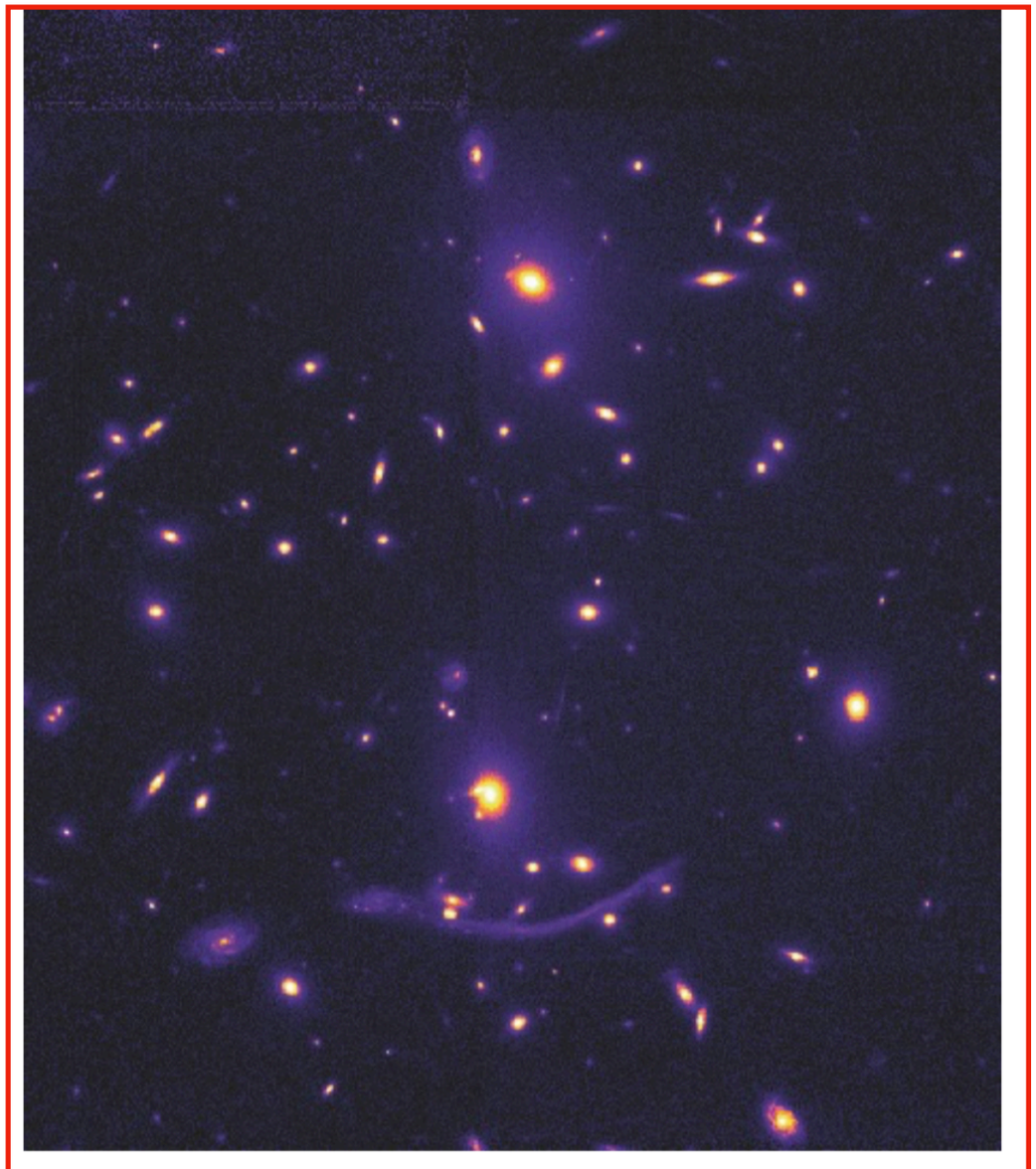

Fig. 6.30. The cluster of galaxies A 370 at redshift $z = 0.375$ is one of the first two clusters in which giant luminous arcs were found in 1986. In this HST image, the arc is clearly visible; it is about 20″ long, tangentially oriented with respect to the center of the cluster which is located roughly halfway between the two bright cluster galaxies, and curved towards the center of the cluster. Only with HST images was it realized how thin these arcs are. In this image, several other lens effects are visible as well, for example a background galaxy that is imaged three-fold. The arc is the image of a galaxy at $z_s = 0.724$

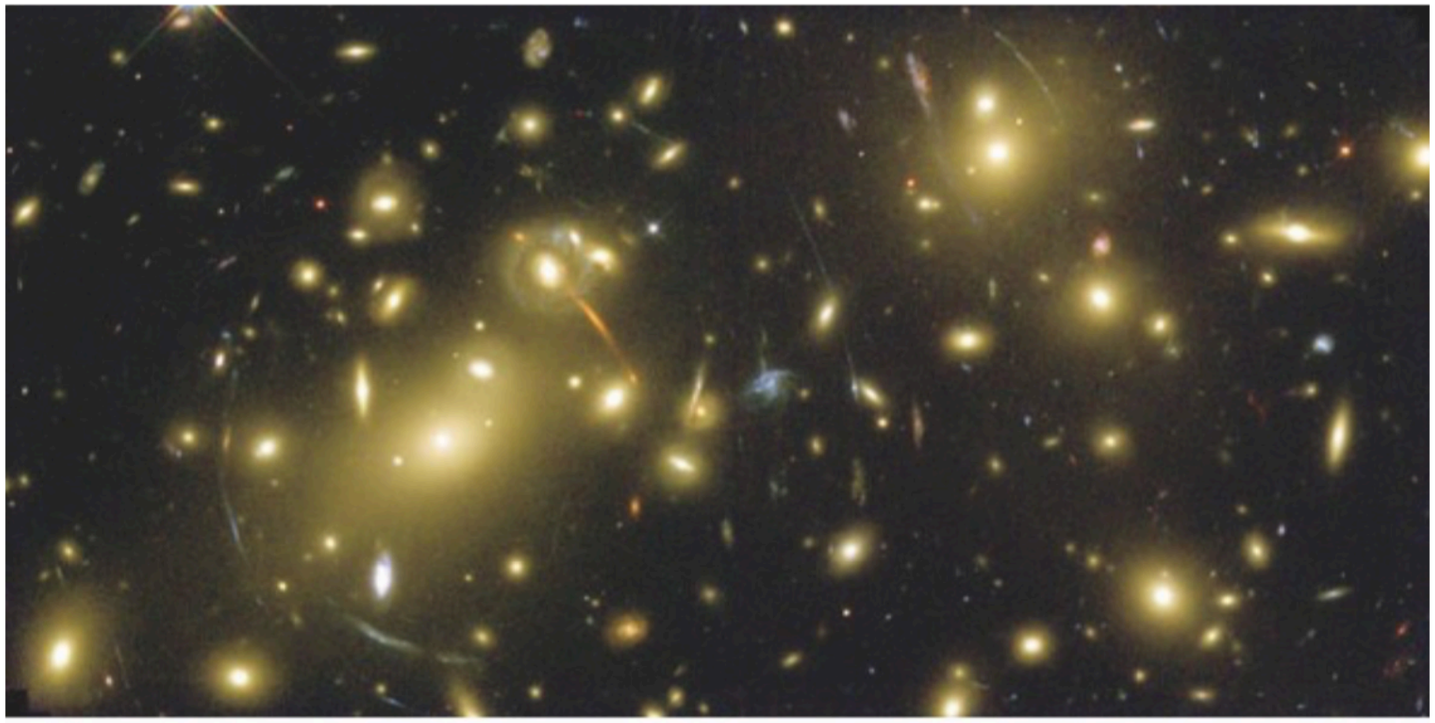

Fig. 6.33. Top image: the cluster of galaxies A 2218 ($z_d = 0.175$) contains one of the most spectacular arc systems. The majority of the galaxies visible in the image are associated with the cluster and the redshifts of many of the strongly distorted arcs have now been measured. Bottom image: the cluster of galaxies Cl 0024+17 ($z = 0.39$) contains a rich system of arcs. The arcs appear bluish, stretched in a direction which is tangential to the cluster center. The three arcs to the left of the cluster center, and the arc to the right of it and closer to the center, are images of the same background galaxy which has a redshift of $z = 1.62$. Another image of the same source was found close to the cluster center. Also note the identical ("pretzel"-shaped) morphology of the images

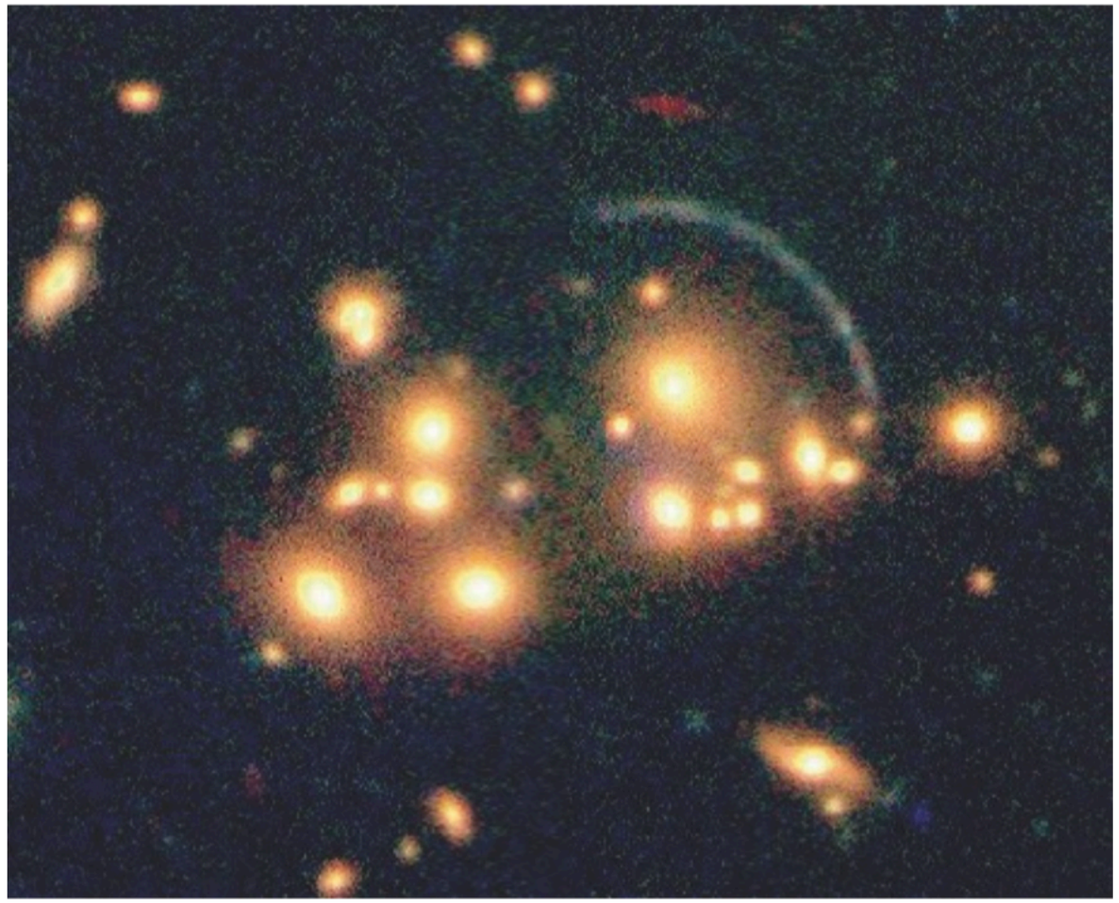

Fig. 6.31. The cluster of galaxies Cl 2244−02 at redshift $z = 0.33$ is the second cluster in which an arc was discovered. Spectroscopic analysis of this arc revealed the redshift of the corresponding source to be $z_s = 2.24$ – at the time of discovery in 1987, it was the first normal galaxy detected at a redshift > 2. This image was observed with the near-IR camera ISAAC at the VLT. Above the arc, one can see another strongly elongated source which is probably associated with a galaxy at very high redshift as well

Fig. 6.34. The cluster of galaxies Abell 1689 has the richest system of arcs and multiple images found to date. In a deep ACS exposure of this cluster more than a hundred such lensed images were detected. Six sections of this ACS image are shown in which various arcs are visible, some with an extreme length-to-width ratio, indicating very high magnification factors

The investigation of galaxy clusters with the gravitational lens method provides a third, completely independent method of determining cluster masses. It confirms that the mass of galaxy clusters significantly exceeds that of the visible matter in stars and in the intracluster gas. We conclude from this result that clusters of galaxies are dominated by dark matter.

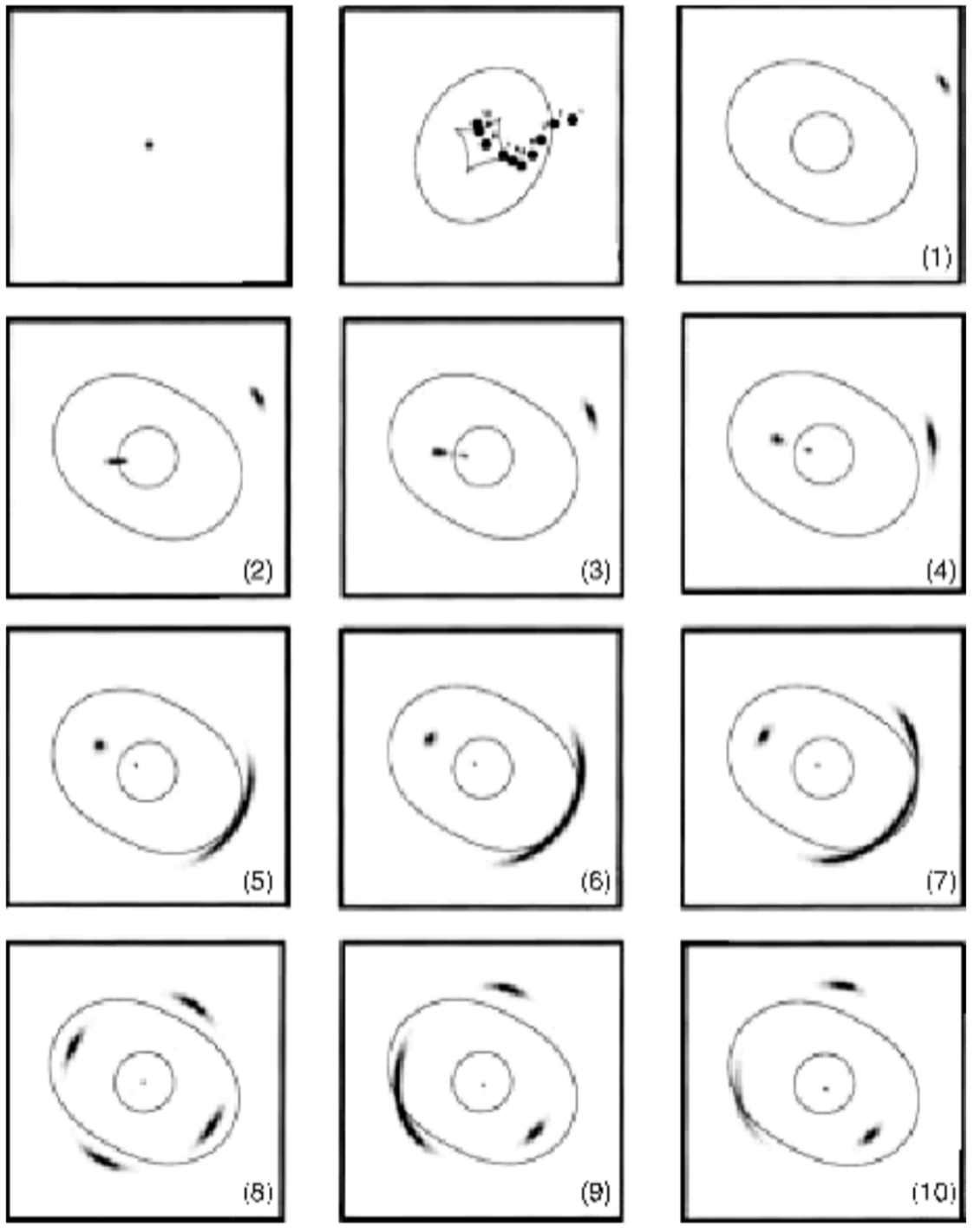

Fig. 6.32. Distortions by the lens effect of an elliptical potential, as a function of the source position. The first panel shows the source itself. The second panel displays ten positions of the source in the source plane (numbered from 1 to 10) relative to the center of the lens; the solid curves show the inner and outer caustics. The remaining panels (numbered from 1 to 10) show the inner and outer critical curves and the resulting images of the source

Clusters of galaxies

6.6 Evolutionary Effects

Today, we are able to discover and analyze clusters of galaxies at redshifts $z \sim 1$ and higher; thus the question arises whether these clusters have the same properties as local clusters. At $z \sim 1$ the age of the Universe is only about half of that of the current Universe. One might therefore expect an evolution of cluster properties.

Luminosity Function. First, we shall consider the comoving number density of clusters as a function of redshift or, more precisely, the evolution of the luminosity function of clusters with z. As Fig. 6.41 demonstrates, such evolutionary effects are not very pronounced, and only at the highest luminosities or the most massive clusters, respectively, does an evolution become visible. This reveals itself by the fact that at high redshift, clusters of very high luminosity or very high mass are less abundant than they are today. The interpretation and the relevance of this fact will be discussed later (see Sect. 8.2.1).

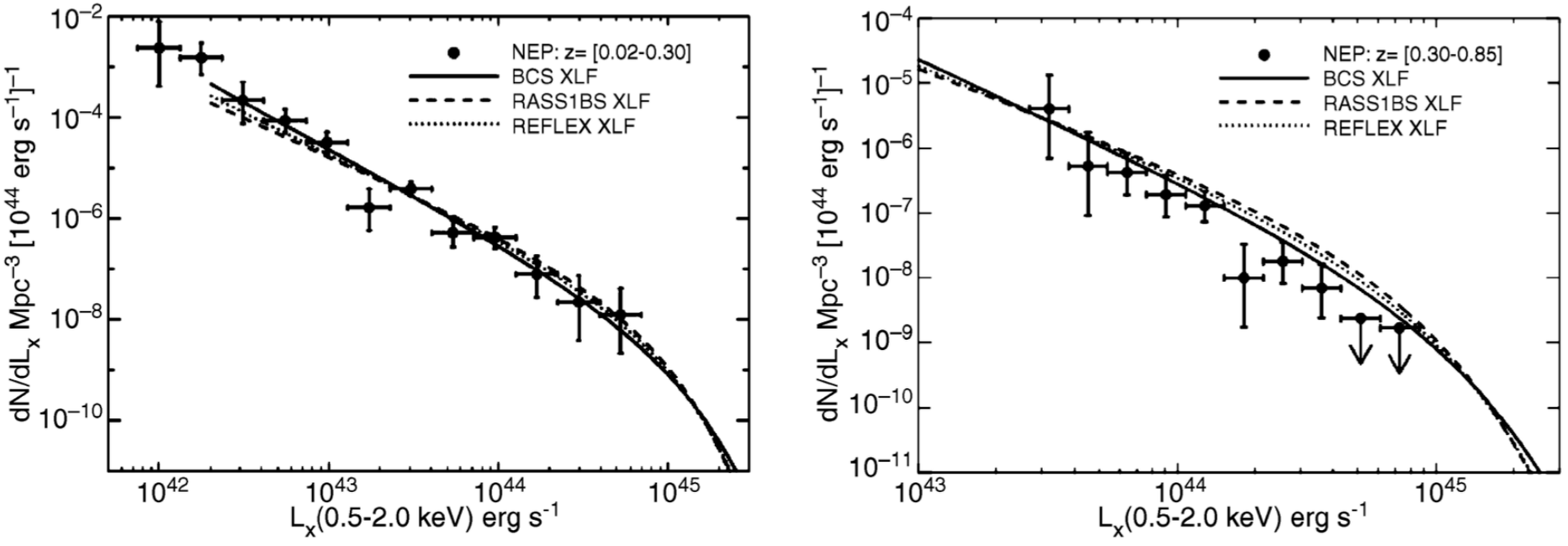

Fig. 6.41. X-ray luminosity function of galaxy clusters, as was obtained from a region around the North Ecliptic Pole (NEP), the region with the longest exposure time in the ROSAT All Sky Survey (see Fig. 6.26). Plotted is $\mathrm{d}N/\mathrm{d}L_\mathrm{X}$, the (comoving) number density per luminosity interval, for clusters with $0.02 \leq z \leq 0.3$ (left panel) and $0.3 \leq z \leq 0.85$ (right panel), respectively. The luminosity was derived from the flux in the photon energy range from 0.5 keV to 2 keV. The three different curves specify the local luminosity function of clusters as found in other cluster surveys at lower redshifts. We see that evolutionary effects in the luminosity function are relatively small and become visible only at high L_X

Clusters of galaxies

Butcher–Oemler Effect. We saw in Chap. 3 that early-type galaxies are predominantly found in clusters and groups, whereas spirals are mostly field galaxies. For example, a massive cluster like Coma contains only 10% spirals, the other luminous galaxies are ellipticals or S0 galaxies (see also Sect. 6.2.9). Besides these morphological differences, the colors of galaxies are very useful for a characterization: early-type galaxies (ellipticals and S0 galaxies) have little ongoing star formation and therefore consist mainly of old, thus low-mass and cool stars. Hence they are red, whereas spirals feature active star formation and are therefore distinctly bluer. The fraction of blue galaxies in nearby clusters is very low.

Butcher and Oemler found that this changes if one examines clusters of galaxies at higher redshifts: these contain a larger fraction of blue galaxies, thus of spirals (see Fig. 6.42). This means that the mixture of galaxies changes over time. In clusters, spirals must become scarcer with increasing cosmic time, e.g., by transforming into early-type galaxies.

A possible and plausible explanation is that spirals lose their interstellar gas. Since they move through the intergalactic gas (which emits the X-ray radiation) at high velocities, the ISM in the galaxies may be torn away and mix with the ICM. This is plausible because the ICM also has a high metallicity. These metals can only originate in a stellar population, thus in the enriched material in the ISM of galaxies.

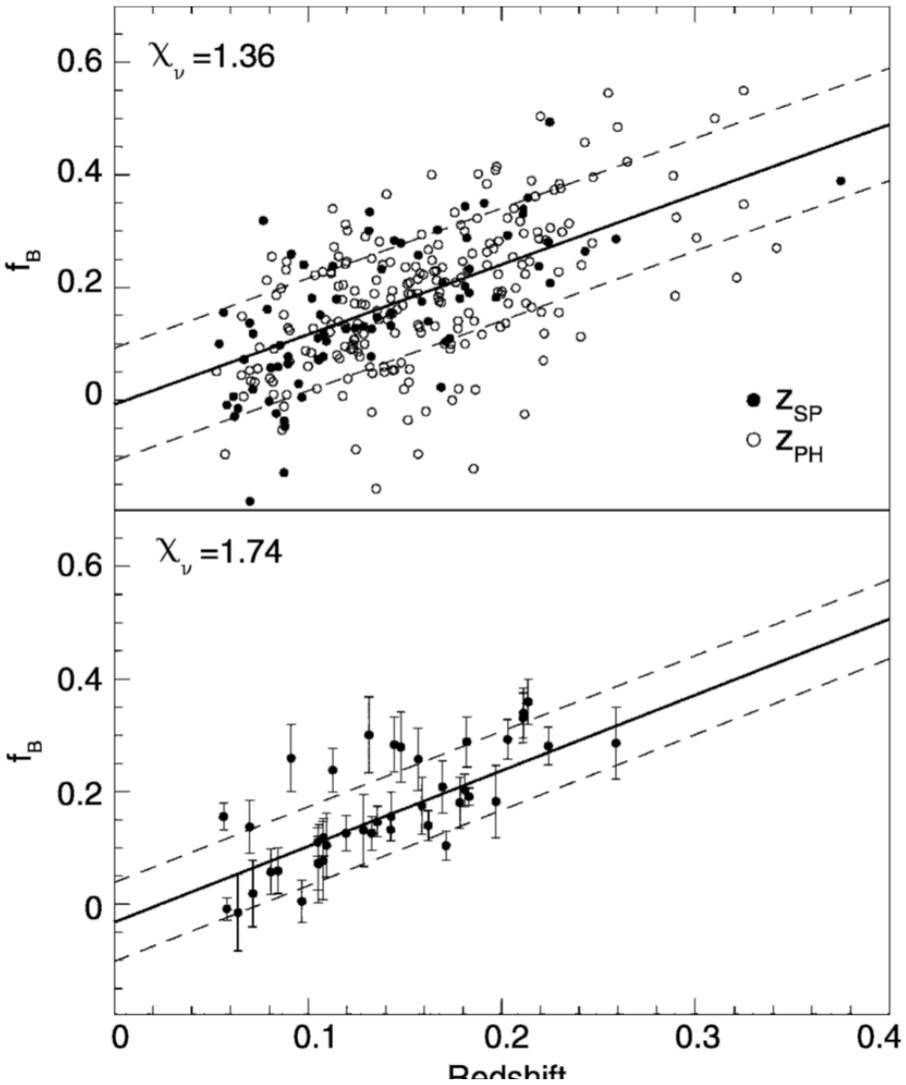

Fig. 6.42. Butcher–Oemler effect: in the upper panel, the fraction of blue galaxies f_b in a sample of 195 galaxy clusters is plotted as a function of cluster redshift, where open (filled) circles indicate photometric (spectroscopic) redshift data for the clusters. The lower panel shows a selection of clusters with spectroscopically determined redshifts and well-defined red cluster sequence. For the determination of f_b, foreground and background galaxies need to be statistically subtracted using control fields, which may also result in negative values for f_b. A clear increase in f_b with redshift is visible, and a line of regression yields $f_b = 1.34z - 0.03$

Clusters of galaxies

Color–Magnitude Diagram. Plotting the color of cluster galaxies versus their magnitude, one finds a very well-defined, nearly horizontal sequence (Fig. 6.43). This red cluster sequence (RCS) is populated by the early-type galaxies in the cluster.

The scatter of early-type galaxies around this sequence is very small, which suggests that all early-type galaxies in a cluster have nearly the same color, only weakly depending on luminosity. Even more surprising is the fact that the color–magnitude diagrams of different clusters at the same redshift define a very similar red cluster sequence: cluster galaxies with the same redshift and luminosity have virtually the same color. Comparing the red sequences of clusters at different redshifts, one finds that the sequence of cluster galaxies is bluer the higher the redshift is. In fact, the red cluster sequence is so precisely characterized that, from the color–magnitude diagram of a cluster alone, its redshift can be estimated, whereby a typical accuracy of $\Delta z \sim 0.1$ is achieved. The accuracy of this estimated redshift strongly depends on the choice of the color filters. Since the most prominent spectral feature of early-type galaxies is the 4000-Å break, the redshift is estimated best if this break is located right between two of the color bands used.

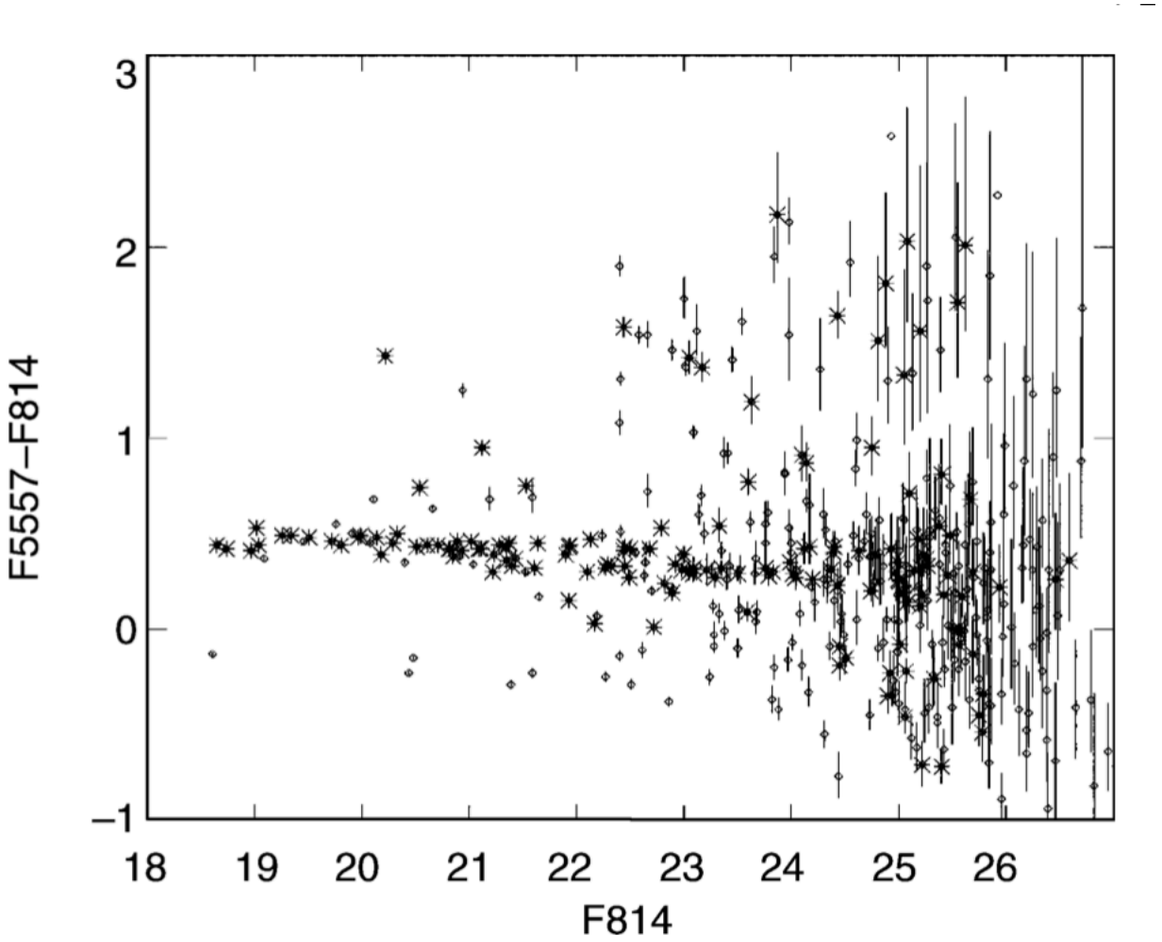

Fig. 6.43. Color–magnitude diagram of the cluster of galaxies Abell 2390, observed with the HST. Star symbols represent early-type galaxies, identified by their morphology, while diamonds denote other galaxies in the field. The red cluster sequence is clearly visible

Clusters of galaxies

This well-defined red cluster sequence is of crucial importance for our understanding of the evolution of galaxies. We know from Sect. 3.9 that the composition of a stellar population depends on the mass spectrum at its birth (the initial mass function, IMF) and on its age: the older a population is, the redder it becomes. The fact that cluster galaxies at the same redshift all have roughly the same color indicates that their stellar populations have very similar ages. However, the only age that is singled out is the age of the Universe itself. In fact, the color of cluster galaxies is compatible with their stellar populations being roughly the same age as the Universe at that particular redshift. This also provides an explanation for why the red cluster sequence is shifted towards bluer colors at higher redshifts – there, the age of the Universe was smaller, and thus the stellar population was younger. This effect is of particular importance at high redshifts. The fact that the color–magnitude diagram of early-type galaxies in clusters is not flat, in that more luminous galaxies are redder, follows from the dependence of galaxy colors on the metallicity of their stellar populations. The higher the luminosity of a galaxy, and thus its stellar mass, the higher its metallicity.

Indeed, from the colors of cluster galaxies it is possible to derive very strict upper limits on their star formation in recent times. The color of cluster galaxies at high redshifts even provides interesting constraints on cosmological parameters – only those models are acceptable which have an age of the Universe, at the respective redshift, larger than the estimated age of the stellar population. One interesting example of this is presented in Fig. 6.44.

Therefore, we conclude from these observations that the stars in cluster galaxies formed at very early times in the Universe. But this does not necessarily mean that the galaxies themselves are also this old, because galaxies can be transformed into each other by merger processes (see Fig. 6.45). This changes the morphology of galaxies, but may leave the stellar populations largely unchanged.

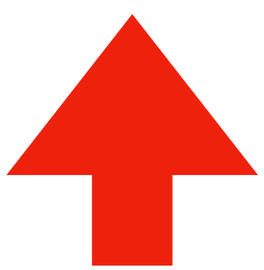

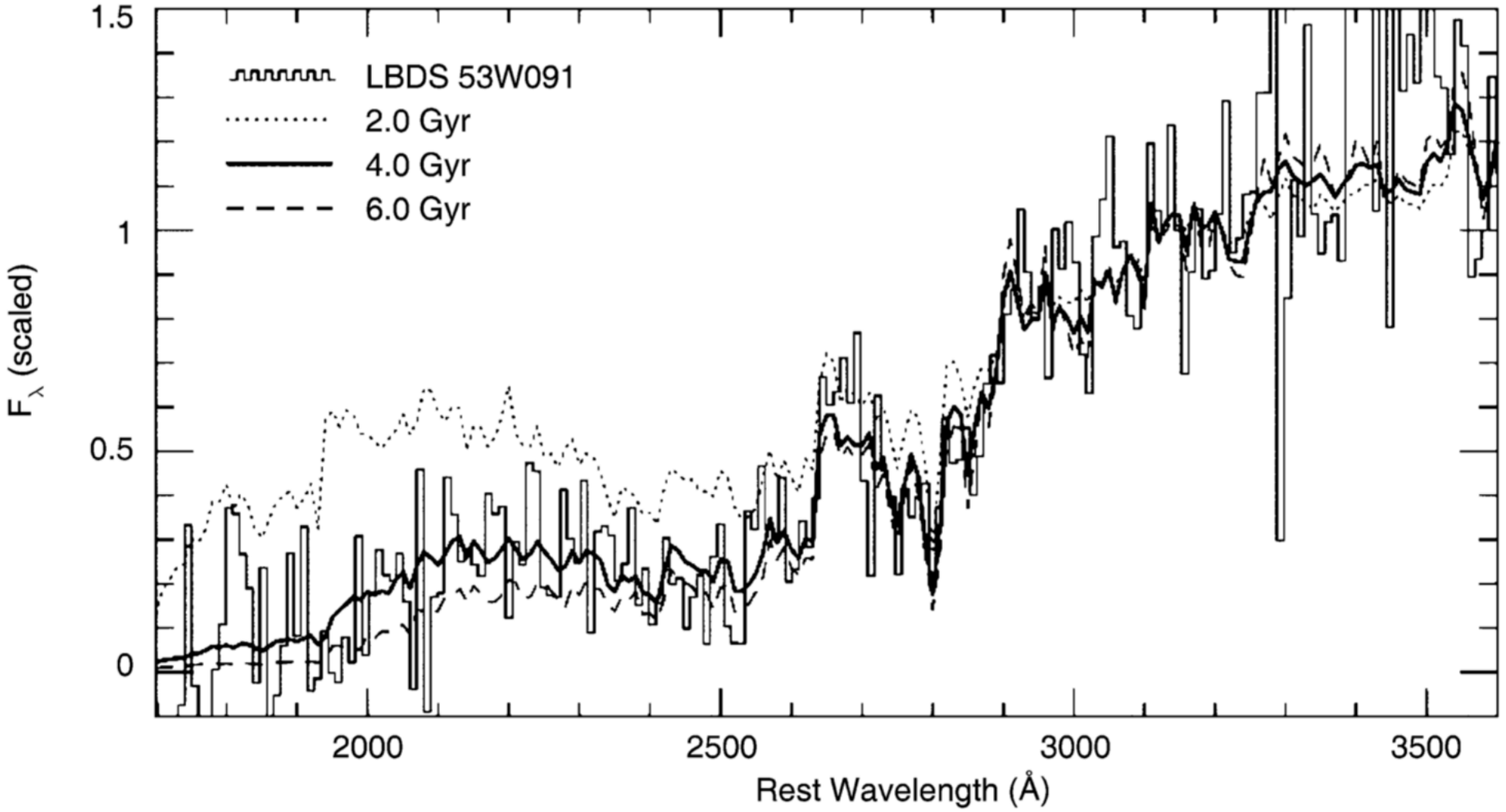

Fig. 6.44. The radio galaxy LBDS 53W091 has a redshift of $z = 1.552$, and it features a very red color ($R - K \approx 5.8$). Optical spectroscopy of the galaxy provides us with the spectral light distribution of the UV emission in the galaxy's rest-frame. The UV light of a stellar population is almost completely due to stars on the upper main sequence – see Fig. 3.38. In the upper left panel, the spectrum of LBDS 53W091 is compared to those of different F stars; one can see that F6 stars match the spectral distribution of the galaxy nearly perfectly. In the bottom panel, synthetic spectra from population synthesis calculations are compared to the observed spectrum. A population with an age of about 4 Gyr represents the best fit to the observed spectrum; this is also comparable to the lifetime of F6 stars: the most luminous (still existing) stars dominate the light distribution of a stellar population in the UV. In combination, this reveals that this galaxy at $z = 1.552$ is at least 3 Gyr old. Phrased differently, the age of the Universe at $z = 1.55$ must be at least 3 Gyr. In the upper right panel, the age of the Universe at $z = 1.55$ is displayed as a function of H_0 and Ω_Λ (for $\Omega_\mathrm{m} + \Omega_\Lambda = 1$). Hence, this single galaxy provides significant constraints on cosmological parameters

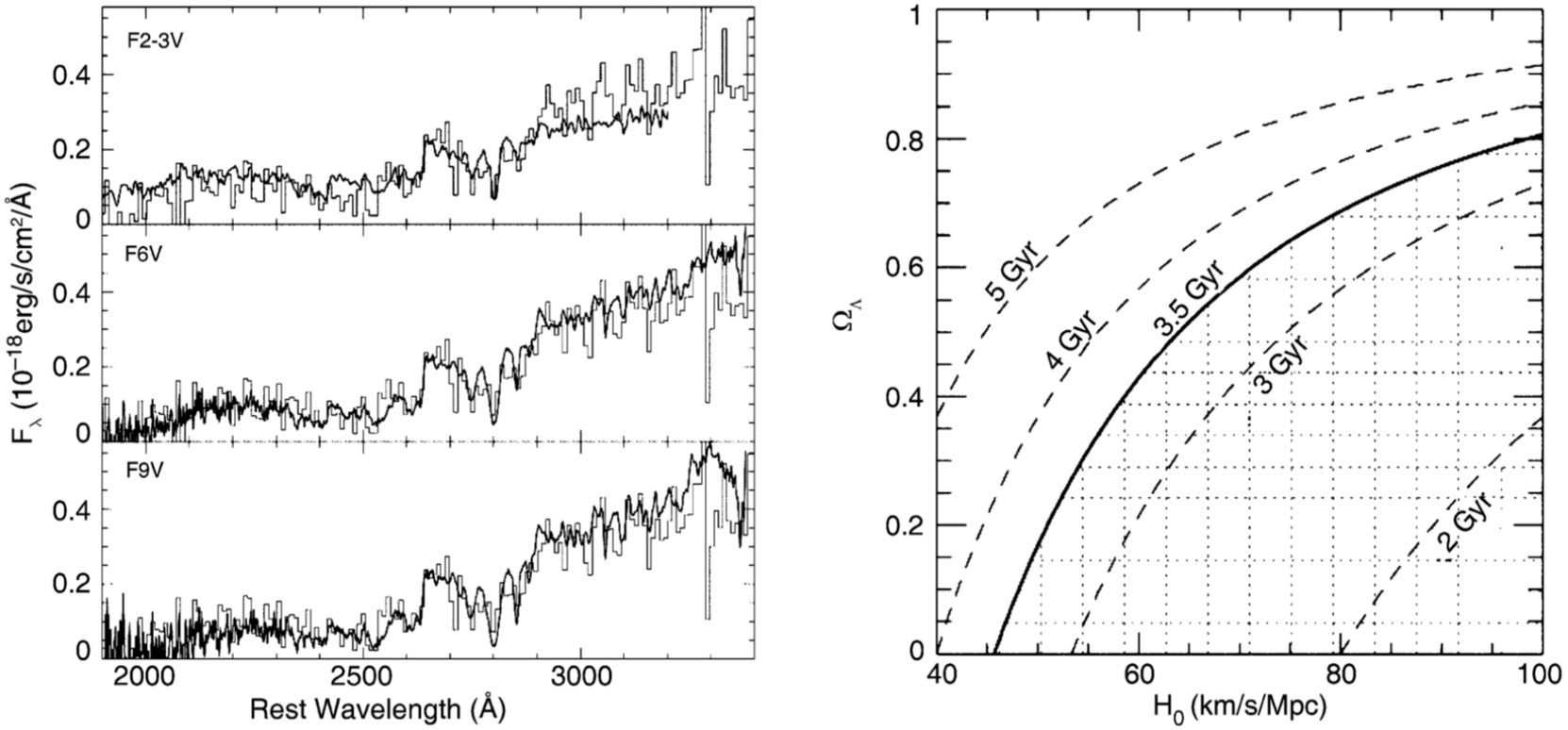

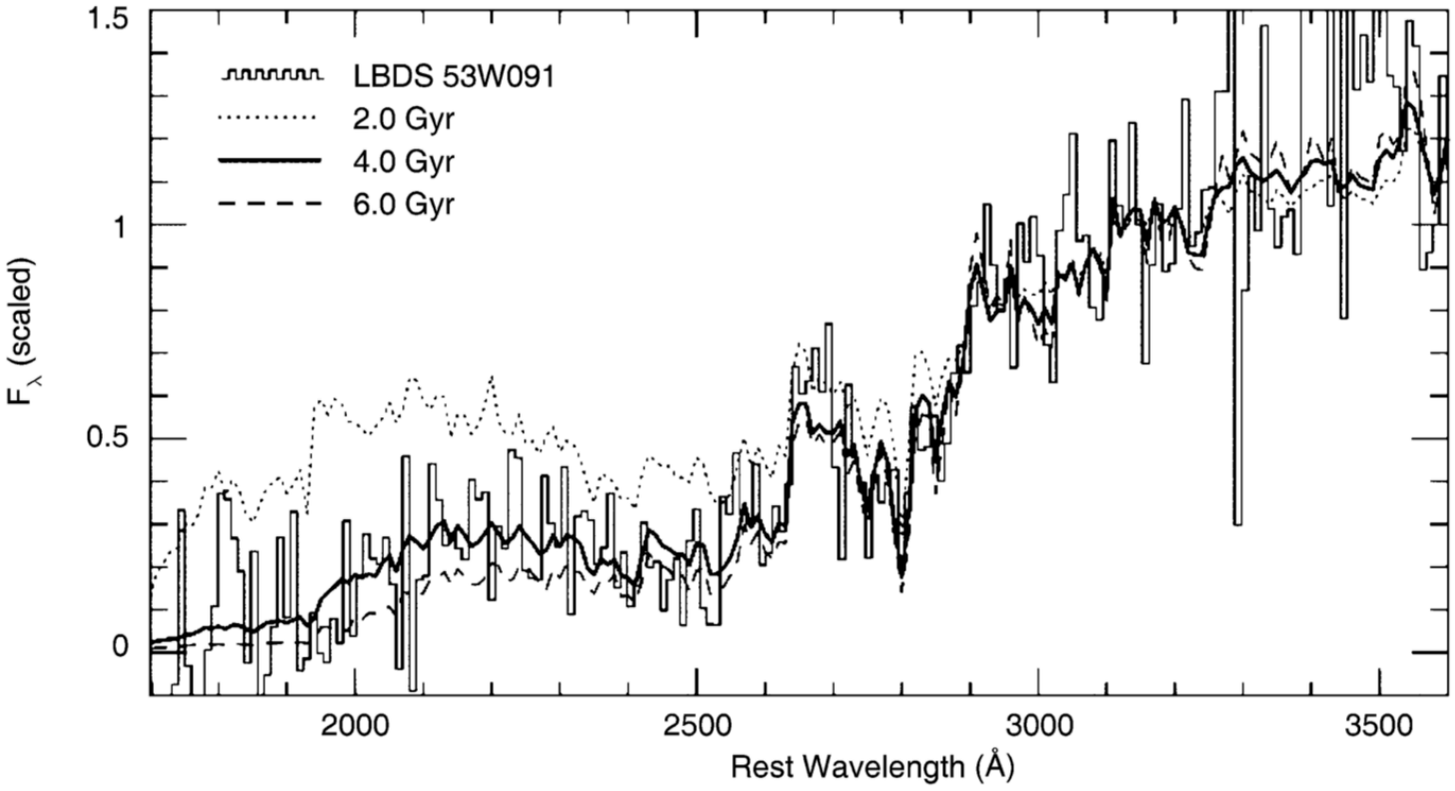

Fig. 6.44. The radio galaxy LBDS 53W091 has a redshift of $z = 1.552$, and it features a very red color ($R - K \approx 5.8$). Optical spectroscopy of the galaxy provides us with the spectral light distribution of the UV emission in the galaxy's rest-frame. The UV light of a stellar population is almost completely due to stars on the upper main sequence – see Fig. 3.38. In the upper left panel, the spectrum of LBDS 53W091 is compared to those of different F stars; one can see that F6 stars match the spectral distribution of the galaxy nearly perfectly. In the bottom panel, synthetic spectra from population synthesis calculations are compared to the observed spectrum. A population with an age of about 4 Gyr represents the best fit to the observed spectrum; this is also comparable to the lifetime of F6 stars: the most luminous (still existing) stars dominate the light distribution of a stellar population in the UV. In combination, this reveals that this galaxy at $z = 1.552$ is at least 3 Gyr old. Phrased differently, the age of the Universe at $z = 1.55$ must be at least 3 Gyr. In the upper right panel, the age of the Universe at $z = 1.55$ is displayed as a function of H_0 and Ω_Λ (for $\Omega_\mathrm{m} + \Omega_\Lambda = 1$). Hence, this single galaxy provides significant constraints on cosmological parameters

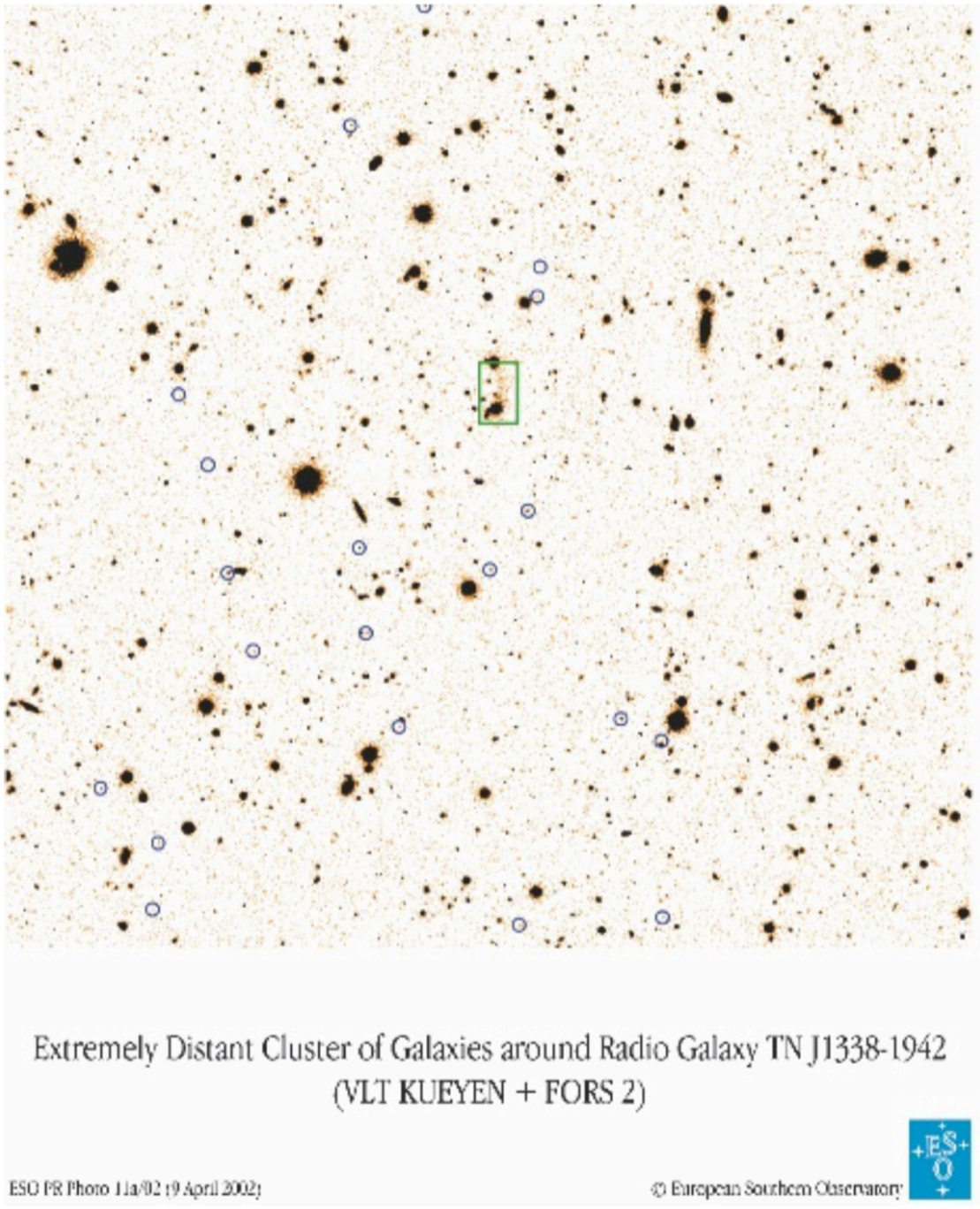

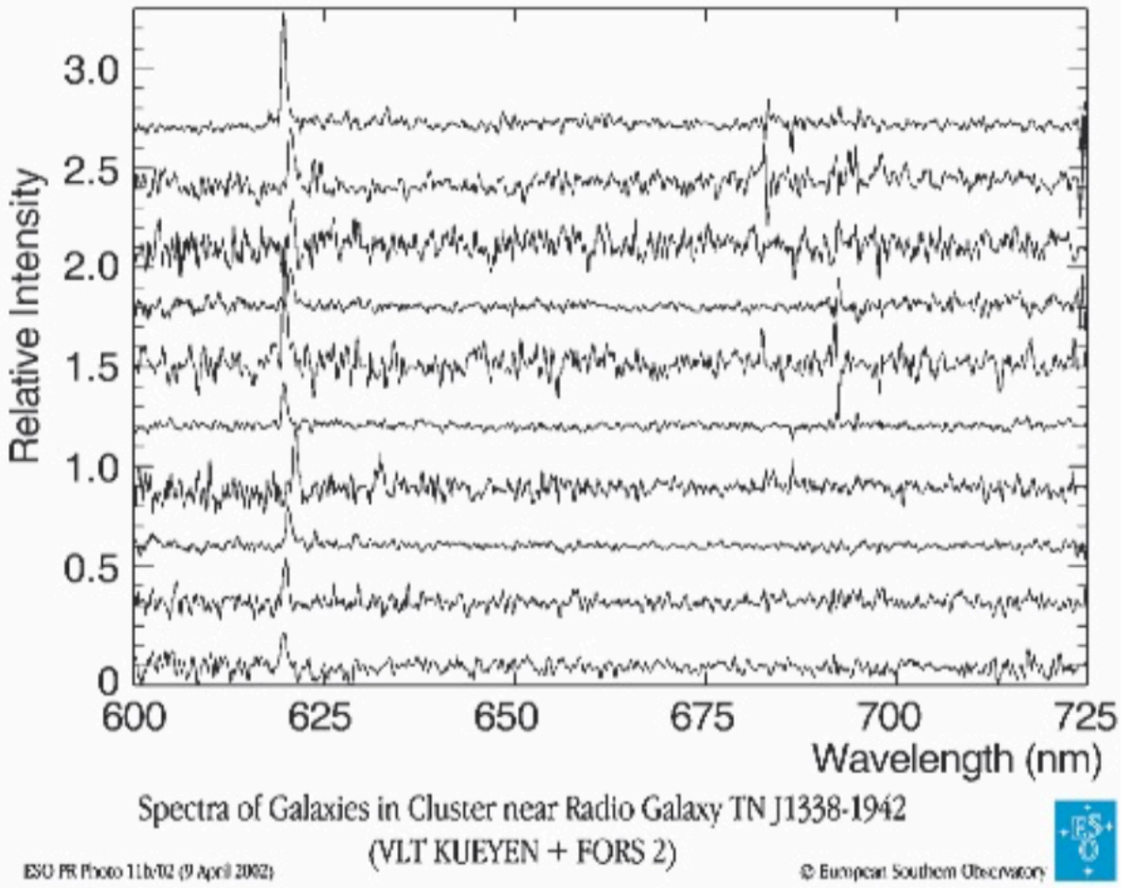

Fig. 6.47. The most distant known group of galaxies. The region around the radio galaxy TN J1338−1942 ($z = 4.1$) was scanned for galaxies at the same redshift; 20 such galaxies were found with the VLT, marked by circles in the left image.

For 10 of these galaxies, the spectra are shown on the right; in all of them, the Lyα emission line is clearly visible. Hence, groups of galaxies were already formed in an early stage of the Universe